NASA TN D-1579

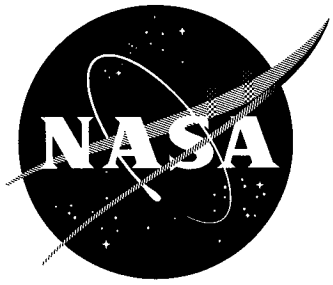

TECHNICAL NOTE

D-1579

PERFORMANCE CAPABILITY OF SINGLE-CAVITY VORTEX GASEOUS NUCLEAR ROCKETS

By Robert G. Ragsdale

Lewis Research Center
Cleveland, Ohio

NATIONAL AERONAUTICS AND SPACE ADMINISTRATION
WASHINGTON

May 1963

NATIONAL AERONAUTICS AND SPACE ADMINISTRATION

TECHNICAL NOTE D-1579

PERFORMANCE CAPABILITY OF SINGLE-CAVITY VORTEX GASEOUS NUCLEAR ROCKETS

By Robert G. Ragsdale

SUMMARY

An analysis was made to determine the maximum powerplant thrust-to-weight ratio possible with a single-cavity vortex gaseous reactor in which all the hydrogen propellant must diffuse through a fuel-rich region. An assumed radial temperature profile was used to represent conduction, convection, and radiation heat-transfer effects. The effect of hydrogen property changes due to dissociation and ionization was taken into account in a hydrodynamic computer program.

It is shown that, even for extremely optimistic assumptions of reactor criticality and operating conditions, such a system is limited to reactor thrust-to-weight ratios of about 1.2×10^{-3} for laminar flow. For turbulent flow, the maximum thrust-to-weight ratio is less than 10^{-3}. These low thrusts result from the fact that the hydrogen flow rate is limited by the diffusion process. The performance of a gas-core system with a specific impulse of 3000 seconds and a powerplant thrust-to-weight ratio of 10^{-2} is shown to be equivalent to that of a 1000-second advanced solid-core system. It is therefore concluded that a single-cavity vortex gaseous reactor in which all the hydrogen must diffuse through the nuclear fuel is a low-thrust device and offers no improvement over a solid-core nuclear-rocket engine.

To achieve higher thrust, additional hydrogen flow must be introduced in such a manner that it will bypass the nuclear fuel. Obviously, such flow must be heated by thermal radiation. An illustrative model of a single-cavity vortex system employing supplementary flow of hydrogen through the core region is briefly examined. Such a system appears capable of thrust-to-weight ratios of approximately 1 to 10. For a high-impulse engine, this capability would be a considerable improvement over solid-core performance. Limits imposed by thermal radiation heat transfer to cavity walls are acknowledged but not evaluated. Alternate vortex concepts that employ many parallel vortices to achieve higher hydrogen flow rates offer the possibility of sufficiently high thrust-to-weight ratios, if they are not limited by short thermal-radiation path lengths.

INTRODUCTION

The use of a reactor employing a fissionable fuel in a gaseous state has received considerable attention as a propulsion unit for a nuclear rocket. Such a device offers the attractive possibility of improved performance by increasing

the maximum propellant-exhaust temperature beyond the limit imposed by the melting point of solid-fuel elements in a heat-transfer nuclear rocket. An elementary consideration of hydrogen-propellant flow rates required for reasonable accelerations (e.g., 10^{-2} g's or greater) and nuclear-fuel-to-hydrogen-mass ratios required for criticality leads immediately to the conclusion that the fuel consumption of a "straight-through" gaseous reactor would be prohibitive. To circumvent this problem, certain flow schemes have been considered that employ hydrodynamic forces to increase the holdup time of the heavy fuel molecules relative to that of the light hydrogen molecules as the mixture passes through the reactor cavity. This increased holdup time decreases the required mass-flow rate of fuel for a given hydrogen flow rate.

Since 1958, the principal effort in gaseous-reactor research has been directed toward a study of a vortex system. In such a device, the propellant (hydrogen) and fissionable fuel (both uranium 235 and plutonium 239 have been considered) are injected at the outer wall of a reactor cavity with a velocity component in the tangential direction. The gases swirl radially inward and are finally exhausted axially. The pressure gradient attendant to this flow field induces pressure diffusion that tends to move the heavier component (fuel) toward the outer wall relative to the light one (hydrogen). This effect is modified by concentration diffusion and radial inflow forces. The steady-state result is that an annular "cloud" forms that is rich in heavy gas. The hydrogen gas diffuses through this region and acquires the nuclear energy release directly by molecular collisions. This general flow pattern is illustrated in figure 1.

Predictably, the emphasis of gaseous-vortex-reactor research has been on the hydrodynamics of the system (refs. 1 to 3). The obvious reason is that if the flow pattern does not result in a critical fuel concentration for acceptable hydrogen-to-fuel flow-rate ratios further considerations are not necessary.

In addition to the basic separation process, other limits of performance capability exist. Some of these performance limits are inherent in any externally moderated gaseous-reactor system, and others apply specifically to a vortex concept. Certain general limitations have been determined for the spectrum of nuclear-rocket systems from all solid-core to all gas-core systems (refs. 4 to 6). A number of recent investigations (refs. 7 to 10) provide a basis for estimating the effects of turbulence in a vortex flow field. Based on certain simplifying assumptions, an analysis has been made of the performance of a turbulent gaseous-reactor system (ref. 11). Some effects of thermal radiation (refs. 12 to 14) and criticality characteristics (refs. 13 and 15) have also been reported, as well as overall system studies (ref. 16).

In view of the combined scope of these various studies, it seems that an evaluation of the most optimistic performance capability of a single-cavity vortex gaseous nuclear rocket is now possible and of value. The goal here is to establish the maximum performance capability and not the most probable. Further, there are, in a sense, two maximum performance levels; one is associated with laminar flow, the other with turbulent flow in the vortex. While it is impossible to say that some future technique will not result in a laminar high-strength vortex, published experimental information indicates that turbulence is most likely to exist.

Finally, a word about the criterion of maximum performance to be used is in order. The system considered herein is one in which all of the nuclear fuel is a gas and is in the reactor cavity. This situation leads to a fixed maximum specific impulse for all gaseous-reactor systems and eliminates the need to consider mission requirements and overall vehicle performance. The hydrodynamics of the system are such that an increase of hydrogen flow rate results in a decrease of average fuel concentration in the reactor cavity; but, to maintain criticality, a larger and heavier reactor is then required. To balance these two effects, the criterion of performance used in this report is the thrust-to-weight ratio of the reactor.

Hydrogen property variations are included in the hydrodynamic computer program for the IBM 7090 digital computer given in appendix B by Muriel B. Eian.

PERFORMANCE LIMITATIONS

It is possible to establish certain limits on a gaseous-vortex-reactor system before making a detailed analysis of the fluid mechanics. Some of these limitations are general in nature and apply to any externally moderated reflected gaseous-reactor system; others apply only to the vortex concept. Some of the limits discussed are arbitrary; in these instances, optimistic values are chosen to establish the maximum bounds of performance.

GENERAL LIMITATIONS

Fuel Consumption

The parameter governing fuel consumption is the hydrogen-to-fuel mass-flow-rate ratio. An upper limit will be established by hydrodynamic and nuclear considerations. If the ratio is too large, fuel concentrations necessary for criticality are not possible. A lower limit on this ratio is somewhat less clearly defined, at least from economic considerations. A ratio of the order of 1000 to 1 has been used as an acceptable value in past considerations. For the purpose of this report, a hydrogen-to-fuel mass-flow-rate ratio of 100 to 1 is taken arbitrarily. Values ranging from 50 to 1 up to 10,000 to 1 were investigated to show the effect of this parameter.

Propellant Molecular Weight

Consumption of nuclear fuel is not the only factor involved in the lower limit of propellant-to-fuel flow ratio. As the fuel-to-hydrogen atom ratio increases, the average molecular weight of the exhaust gas obviously increases. An upper limit on fuel concentration is reached when the increase in the average molecular weight begins to decrease the specific impulse significantly. The exhaust gas average molecular weight $\overline{M}$ can be easily expressed in terms of the hydrogen-to-fuel mass-flow-rate ratio and the fuel-to-hydrogen molecular-weight ratio:

$$\overline{M} = \frac{\frac{M_2}{M_1}\left(1 + \frac{w_1}{w_2}\right)}{1 + \frac{w_1}{w_2}\frac{M_2}{M_1}} M_1$$

For the situations considered here, $(w_1/w_2)(M_2/M_1)$ is sufficiently large so that

$$\overline{M} \simeq \left(1 + \frac{1}{\frac{w_1}{w_2}}\right) M_1$$

The 100 to 1 mass-flow-rate ratio selected from economic considerations will result in approximately a 1-percent increase in propellant molecular weight. The resulting 1/2-percent decrease in specific impulse certainly does not represent a serious limitation on performance, and the mass-flow-rate ratio of 100 to 1 will give optimistic results. (All symbols are defined in appendix A.)

Nucleonics

There are two limitations that arise from the nucleonics of gaseous reactors. The first of these is the pressure required for criticality. With all other parameters fixed, virtually any reactor scheme can be made critical by simply operating at whatever system pressure is required for criticality. The choice here, again arbitrary, will be a maximum pressure in the reactor cavity of 500 atmospheres. Since the contemplated operating pressure of current solid-fuel reactors is considerably smaller, this choice must be considered optimistic.

A more subtle limitation exists due to gamma and neutron heating of the solid materials surrounding the reactor cavity. This effect has been considered in detail elsewhere (ref. 4) and is only briefly reiterated here. The fraction of the total power generation, which results from gamma and neutron heating, and thermal radiation to the cavity walls must be removed from the solid regions by the hydrogen before it enters the reactor cavity. The resulting enthalpy rise of the hydrogen in the solid region of a gaseous reactor clearly cannot exceed the total rise possible in a solid-core-reactor system. This, then, fixes the maximum possible enthalpy gain available to the hydrogen in a gas-core system, as explained in the following paragraph.

It is assumed herein that the combined effects of nuclear and thermal radiation result in the deposition of 10 percent of the total power in the solid region. Further, it is assumed that the hydrogen enters the reactor cavity at 5000° R. These conditions result in a maximum possible exhaust temperature of 15,000° to 20,000° R, depending on pressure, and a specific impulse of approximately 3000 seconds. The only possibility of obtaining a higher specific impulse is through the use of a radiator to dispose of the additional solid-region heat (ref. 4).

Heat Transfer to Walls

Two aspects of gaseous-reactor heat transfer are mentioned here, although no resulting limitations are included in this study. The first limit is imposed by the allowable cavity wall temperature. Any system that proposes to contain gas at temperatures of the order of 15,000° R is faced with thermal-radiation problems; these have been treated in other investigations (refs. 12 to 14). Another heat-transfer problem is associated with exhaust-nozzle cooling. Although relatively unexamined to date, this problem may well place a serious limitation on any gaseous-reactor system.

VORTEX-SYSTEM LIMITATIONS

Geometry

The performance limitation imposed by reactor geometry arises from the fact that the separation process improves with decreasing mass flow of hydrogen per unit cavity length. The combination of criticality and hydrodynamic considerations suggests that the reactor should be composed of many small-diameter tubes in order to obtain a high hydrogen mass flow (refs. 1 and 17); however, the inlet headers, exhaust ducting, and short thermal radiation path lengths associated with small diameter, large length-to-diameter ratio (L/D) vortex tubes pose extremely severe heat-transfer problems. All the findings of this report, as the title implies, are for a single-cavity vortex gaseous reactor.

Hydrodynamics

For given values of critical fuel density and maximum operating pressure, the hydrodynamic relations prescribe a maximum hydrogen flow rate per unit cavity length. The assumptions utilized in reference 1 gave a value of approximately 0.01 pound per second per foot. The two flow regions to be considered herein, laminar and turbulent, will result in one maximum for each. This maximum hydrogen flow rate, however, will not necessarily yield the highest thrust-to-weight ratio. Two other limitations imposed by hydrodynamics are: (1) axial choking at the vortex exit, and (2) nonequilibrium nozzle expansion. The limit of choked flow in the vortex exhaust is included in the analysis of this report, and equilibrium expansion is assumed.

ANALYSIS

An analysis of the hydrodynamics, vortex axial choking, criticality, and performance characteristics of a vortex gaseous nuclear rocket is presented herein, in that order. The general development of the hydrodynamic relations follows that presented in reference 2. Hydrogen properties and the hydrodynamic computer program are discussed in detail in appendixes B and C.

ASSUMPTIONS

The assumptions utilized in the following analysis are listed here for convenience. The more important ones are also noted at the point in the analysis where they are introduced.

(1) $\partial/\partial\theta = \partial/\partial z = 0$ (except in vortex core where axial mass flow varies linearly with axial position)

(2) Steady-state conditions exist

(3) Perfect gas law is obeyed

(4) Hydrogen gas species are present in equilibrium amounts

(5) External body forces are negligible

(6) Thermal diffusion is small compared with pressure and concentration diffusion

(7) Radial velocities are small compared with tangential velocities

(8) μ and $\rho\epsilon$ do not vary with radial position

(9) Laminar diffusion coefficient is given by Gilliland expression

(10) Turbulent flow is described by laminar equations if μ is replaced by $\rho\epsilon_{mo}$ and $(D_{12} + \epsilon_{ma})$ is substituted for D_{12}

(11) Turbulence affects concentration diffusion but not pressure diffusion

(12) Combined effect of molecular collision heating, conduction, and radiation heat transfer is adequately represented by an assumed radial temperature profile $t(x)$

(13) Reactor criticality is unaffected by a nonuniform fuel distribution or presence of structural material

(14) Equilibrium expansion occurs in exhaust nozzle

(15) Ten percent of total power generation is deposited in moderator-reflector region

(16) The maximum possible hydrogen peripheral Mach number is 1.0

(17) Fuel gas does not ionize

(18) Axial choking occurs at density conditions in vortex at exit radius

(19) Maximum permissible pressure at vortex perimeter is 500 atmospheres

(20) Temperature of hydrogen entering reactor cavity is 5000° R

HYDRODYNAMICS

Laminar Flow

The Navier-Stokes equations of motion for compressible vortex flow are as follows:

$$\frac{dp}{dr} = \frac{\rho}{g}\frac{v^2}{r} \tag{1}$$

$$\rho u \frac{dv}{dr} + \rho u \frac{v}{r} = \mu\left[\frac{d}{dr}\left(\frac{dv}{dr} - \frac{v}{r}\right) + \frac{2}{r}\left(\frac{dv}{dr} - \frac{v}{r}\right)\right] \tag{2}$$

These equations are consistent with assumptions (1), (2), (7), and (8).

In lieu of an energy equation, the static-temperature profile will be represented by an assumed distribution (assumption (12)) of the form

$$t(x) = a_1 + a_2x + a_3x^2 + a_4x^3 + a_5x^4 \tag{3}$$

The constants are chosen such that temperature increases monotonically from 5000° R at the outer radius to a maximum value at the center of the vortex and that the temperature gradient is essentially zero at the center. In addition, the temperature increases to near its maximum value at a radius ratio larger than that of the maximum uranium concentration for all cases considered. This would actually occur because conduction and radiation would tend to increase the hydrogen temperature before it entered the fuel-rich region.

An alternate approach would be to assume that the volumetric heat-generation rate is proportional to the concentration of fissionable gas (ref. 1). Since a rigorous treatment of radiative heat transfer would introduce considerable complexity to an already cumbersome computer program, the compromise represented by equation (3) is considered entirely adequate for this analysis.

The continuity equation for the annular region $r_o \geq r \geq r_n$ is

$$\frac{d}{dr}\rho u r = 0 \tag{4}$$

The assumption of a perfect gas gives

$$p = \frac{\rho R t}{M} \tag{5}$$

as the equation of state.

By virtue of assumptions (5) and (6), the diffusion equation is

$$u_1 - u_2 = \frac{-n^2}{n_1 n_2} D_{12}\left[\frac{d\left(\frac{n_1}{n}\right)}{dr} + \frac{n_1 n_2 (M_2 - M_1)}{n\rho} \frac{1}{p} \frac{dp}{dr}\right] \tag{6}$$

where $n = n_1 + n_2$.

A laminar Reynolds number is defined in terms of the radius and radial velocity as

$$Re_l = - \frac{\rho u r}{\mu} \tag{7}$$

The negative sign is used so that a positive Reynolds number is associated with flow that is radially inward. The continuity equation and assumption (8) result in a Reynolds number that does not vary with radial position.

Integration of the continuity equation for the annular region yields

$$-\rho u r = \frac{w}{2\pi} = \frac{w_1 + w_2}{2\pi} \tag{8}$$

where w is the total mass flow per unit axial length. In the core of vortex $r_n \geq r \geq 0$, the assumption of constant mass flow per unit area in the axial direction gives the continuity relation (ref. 10) as

$$\rho u r = \rho_n u_n r_n \left(\frac{r}{r_n}\right)^2 \tag{9}$$

The tangential velocity profile is obtained by integrating equation (2) with the boundary conditions $v(r_o) = v_o$ and $v(0) = 0$:

$$v = \left(\frac{v_o}{x}\right) \sqrt{\psi} \tag{10}$$

where x is the radius ratio r/r_o, and ψ is a function of x, x_n, and Re_l. In the vortex core, ψ is given by

$$\psi = \left\{\frac{x_n}{v_o'}\left[\frac{1 - e^{-Re_l/2(x/x_n)^2}}{1 - e^{-Re_l/2}}\right]\right\}^2 \tag{11}$$

and

$$\frac{x_n}{v_o'} = \left[1 + \left(\frac{1}{2 - Re_l}\right)\left(\frac{Re_l}{e^{Re_l/2} - 1}\right)\left(x^{Re_l - 2} - 1\right)\right]^{-1} \tag{11a}$$

In the annular region, ψ is given by

$$\psi = \left(\frac{x_n}{v_o'}\right)^2 \left[(1 - C)^2 + \frac{2(C - C^2)}{\left(\frac{x}{x_n}\right)^{Re_l - 2}} + \frac{C^2}{\left(\frac{x}{x_n}\right)^{2Re_l - 4}} \right] \tag{12}$$

where

$$C \equiv \left(\frac{1}{2 - Re_l}\right)\left(\frac{Re_l}{e^{Re_l/2} - 1}\right) \tag{12a}$$

and x_n/v_o' is given by equation (11a).

It is of interest to note that when $\mu \to 0$, the function $\psi \to 1$, and equation (10) gives the usual $1/r$ variation of tangential velocity for a potential vortex. In fact, the $1/r$ profile is closely approximated for any Re_l greater than about 10.

The pressure gradient from equation (1) may be written in the form

$$\frac{d}{dx}\left(\frac{p}{p^*}\right) = \frac{(y_1 M_1 + y_2 M_2)v^2}{gRtx}\left(\frac{p}{p^*}\right) \tag{13}$$

The pressure is normalized to p^*, its value at some radius ratio x^*. In this analysis, x^* is the radius ratio at which the mole fraction of the heavy component y_2 is at a maximum y_2^*. The numerical integration procedure will begin at x^* and proceed to $x = 1$, then go from x^* to x_n, and, finally, from x_n to 0. The computer program is discussed in detail in appendix B.

The diffusion equation may be written in terms of y_2 using equations (1), (5), (6), and (8) as follows:

$$\frac{dy_2}{dx} = -\frac{\alpha_2(by_2 - 1)}{x} + \frac{\beta(y_2 - y_2^2)}{x^3} \tag{14}$$

where

$$\alpha_2 \equiv \frac{w_2}{2\pi M_2 D_{12} n} \qquad \beta \equiv \frac{(M_2 - M_1)v_o^2 \psi}{gRt}$$

$$b \equiv 1 + \frac{w_1}{w_2}\frac{M_2}{M_1}$$

The product of the laminar diffusion coefficient and the molecular density is calculated from the Gilliland relation:

$$D_{12}n = \frac{2.62\times10^{-6}\sqrt{t}\left(\frac{1}{M_1} + \frac{1}{M_2}\right)^{1/2}}{\left(V_1^{1/3} + V_2^{1/3}\right)^2}$$

The molecular volumes of hydrogen and uranium were taken to be 14.3 and 105 cubic centimeters per gram mole, respectively. The other hydrogen properties, molecular weight, specific heat, ratio of specific heats, and composition were allowed to vary with vortex radius as a function of temperature and pressure. The hydrogen property variation is discussed in appendix C.

The mole fraction of the heavy component y_2 is related to mass-flow and radial-velocity ratios in the following manner:

$$y_2 = \frac{1}{1 + \frac{w_1}{w_2}\frac{M_2}{M_1}\frac{u_2}{u_1}} \tag{15}$$

The system of equations required to describe the hydrodynamic separation process is now complete and is given by equations (3), (5), either (8) or (9), (10), (13), and (14). The two nonlinear differential equations were solved by the Runge-Kutta numerical method. The boundary condition for equation (13) is $p = p^*$ at $x = x^*$. The boundary condition for equation (14) is $dy_2^*/dx^* = 0$. The implications of this boundary condition are discussed in RESULTS AND DISCUSSION.

Total temperature and pressure are calculated from

$$T = t + \frac{v^2}{2c_p gJ} \tag{16}$$

$$P = p\left[1 + \left(\frac{\gamma - 1}{2}\right)\frac{(y_1M_1 + y_2M_2)v^2}{\gamma gRt}\right]^{\gamma/(\gamma-1)} \tag{17}$$

Turbulent Flow

The hydrodynamic relations for a turbulent vortex are obtained by substituting $\rho\epsilon_{mo}$ for μ and $D_{12} + \epsilon_{ma}$ for D_{12} into the laminar equations with one exception in the diffusion expression. For turbulent flow, the Reynolds number is defined as

$$Re_t \equiv - \frac{\rho u r}{\rho \epsilon_{mo}} \tag{18}$$

The tangential velocity profile is still given by equation (10), but ψ is now evaluated with a turbulent Reynolds number. The eddy diffusivity for momentum transfer ϵ_{mo} can be calculated from equation (18) for a given value of Re_t. For all the turbulent-flow considerations in this report, $\epsilon_{mo}/\epsilon_{ma} = 1$.

It will be assumed herein, as it was in reference 2, that equation (14) is valid for turbulent diffusion if $(D_{12} + \epsilon_{ma})$ is substituted for D_{12} in the concentration-gradient term of equation (6). The coefficient of the pressure-diffusion term is unchanged, but that does not imply that pressure diffusion is unaffected by turbulence. The coefficient is unchanged, but the effect of turbulence is exhibited in the pressure gradient.

With this assumption, the turbulent-diffusion equation becomes

$$\frac{dy_2}{dx} = \frac{D_{12}}{D_{12} + \epsilon_{ma}} \left[\frac{-\alpha_2(by_2 - 1)}{x} + \frac{\beta(y_2 - y_2^2)}{x^3} \right] \tag{19}$$

The functions α_2, b, and β are the same as those given for equation (14).

AXIAL CHOKING

An upper limit on hydrogen flow rate is placed by hydrodynamic choking at the vortex axial exit. The hydrogen flow rate per unit length required for choked flow w_{ch} is given by

$$w_{ch} = \frac{v_s A_n \rho_n}{L} \tag{20}$$

where v_s, the velocity of sound in hydrogen, and the density ρ_n are evaluated at the vortex-exit radius r_n. This approximation will result in an optimistic (high) value for w_{ch}; the average density in the vortex exit will be less than the value at r_n because of the pressure gradient in the core.

For temperatures and pressures in this study, γ for an equilibrium mixture of hydrogen species varies less than 1 percent from 1.05. With this value and $A_n = 2\pi r_n$, equation (20) can be written in the following form for $t_n = 19,860^\circ$ R:

$$\frac{w_{ch}}{r_o} = 3.71\, x_n^2 \left(\frac{p_n M_{1,n}}{L/D} \right) \tag{21}$$

where $M_{1,n}$ is the average molecular weight of the propellant at p_n and T_n.

CRITICALITY

The critical mass values used in this report are taken from the results of a two-dimensional analysis of gas-core cavity reactors (ref. 15). Critical density as a function of reactor radius for cavity length-to-diameter ratios of 1/2, 1, and 2 was computed herein from cylindrical reactor critical mass estimates based on a buckling analogy presented in reference 15. These criticality requirements are for a reactor cavity uniformly filled with uranium 235 and completely surrounded by a 70° F heavy water (D_2O) moderator-reflector region.

This choice of moderator material admittedly results in a criticality requirement that is more optimistic than realistic. Estimates of critical density for two other reactor systems were obtained by using multiplying factors obtained from reference 15. One of these systems is a uranium 235 fueled cavity surrounded by graphite at 5300° F, and the other is a plutonium 239 fueled cavity with a 5300° F graphite moderator.

PERFORMANCE

Thrust-to-reactor weight is used as the criterion of reactor performance. This ratio is given by:

$$\frac{F}{W_R} = \frac{w_1 L I_{sp}}{W_R} \tag{22}$$

It is assumed that the reactor weight is that of the moderator reflector. In equation (22), L is the length of the reactor cavity; it does not include the end reflectors.

RESULTS AND DISCUSSION

GENERAL PERFORMANCE CHARACTERISTICS

Comparison With Solid-Core Performance

It is worthwhile to investigate some general characteristics of gas-core nuclear rockets that are independent of the hydrodynamics of a specific system. The trade-off between specific impulse and powerplant thrust-to-weight ratio, for example, is of interest because a gas-core system may provide a higher impulse but lower thrust-to-weight ratio than a solid-core heat-transfer rocket.

Figure 2, which is taken from information in reference 18, shows the effect of powerplant thrust-to-weight ratio on the specific impulse required for a seven-man 460-day Venus mission. The parameter here is the ratio of vehicle weight for a system under consideration to that of an advanced (I_{sp} = 1000 sec) solid-core system. The curves of figure 2 show that a gaseous-reactor scheme that provides a specific impulse of 3000 seconds must have a powerplant thrust-to-weight ratio of about 10^{-2} in order to perform the same mission as a solid-

core rocket of the same gross weight. A thrust-to-weight ratio of approximately 2 with a 3000-second impulse would allow the vehicle weight to be one-half that of a solid-core system. So, the general conclusion here is that a gas-core system must offer reactor thrust-to-weight ratios greater than 10^{-2} in order to merit consideration.

The performance advantage of a 3000-second-impulse engine with a thrust-to-weight ratio greater than 10^{-1} does not have to be utilized in terms of decreased vehicle weight. Figure 3 shows the decrease in trip time that is possible because of increased specific impulse for a constant (1.7×10^6 lb) vehicle weight. The 460-day trip time required by a 1000-second solid-core rocket can be reduced significantly to 150 days for a 3000-second gas-core system. This gain over a solid-core rocket is probably of more value than a gain in terms of decreased vehicle weight.

Attainable Specific Impulse

Because a gaseous nuclear rocket can potentially produce extremely high propellant temperatures, it is of interest to consider briefly what specific impulses are possible with such systems, though a fixed impulse of 3000 seconds is used in this study. Since specific impulse is simply a measure of energy content, specification of the reactor temperature and pressure determines the equilibrium impulse available from hydrogen exhausting to a vacuum.

Figure 4 shows the equilibrium specific impulse in vacuum for temperatures from 5000° to 35,000° R and reactor pressures of 1, 10, and 100 atmospheres, as calculated from enthalpy values given in reference 19. As pointed out in PERFORMANCE LIMITATIONS, the fraction of the total enthalpy rise that the hydrogen must acquire to remove the energy deposited in the solid regions of a reactor limits the total enthalpy rise possible. This parameter φ is shown in figure 4 for an assumed hydrogen temperature of 5000° R at the inlet to the reactor cavity. If 10 percent of the total reactor power must be removed from the solid regions, the maximum hydrogen exhaust temperature is between 17,000° and 19,000° R. This gives a specific-impulse range from 2900 to 3200 seconds. For a φ of 20 percent, hydrogen exhaust temperatures are limited to 7500° to 10,000° R, with impulses from 2050 to 2275 seconds. Though values of 15 to 20 percent solid-region heat generation are probably more realistic, a value of 10 percent is assumed possible, and a constant specific impulse of 3000 seconds was used herein for all performance calculations.

A vortex gaseous reactor enjoys one advantage as a result of the large radial pressure gradient attendant to a vortex flow field. The radial decrease in pressure allows dissociation and ionization of the hydrogen to occur at a lower temperature (fig. 5). For a given wall pressure, the average exhaust temperature necessary to obtain an enthalpy rise that is 10 times that of a solid-core rocket (operating at the same wall pressure) decreases at lower exhaust-nozzle pressure. For example, a uniform reactor pressure of 100 atmospheres would require a hydrogen average exhaust temperature of 16,750° R to give a specific impulse of around 3000 seconds. A vortex reactor operating at a wall pressure of 100 atmospheres and an exhaust pressure of 0.1 atmosphere would only require an exhaust temperature of 14,950° R for the same impulse.

Reactor Criticality

The criticality requirements of an externally moderated cavity reactor are shown in figure 6. These curves were computed from results presented in reference 15 and are for cylindrical reactors with side and end moderator reflectors 100-centimeters thick. The three solid-line curves of critical density against cavity radius are for a uranium 235 fuel and a 70° F D_2O moderator. For high-temperature operation, heavy water is obviously an unrealistic choice but was used for the calculations of this report in order to assure an optimistic evaluation of performance. The criticality requirements of more practical systems that utilize 5300° F graphite as a moderator and either plutonium 239 or uranium 235 as a nuclear fuel are shown for comparison, but were not used. The curves in figure 6 are for a reactor cavity uniformly filled with fuel, and it is assumed here that no increase in critical mass would result from a nonuniform distribution, though in fact this would be true.

Reactor Geometry

It is also possible to determine some general effects of reactor geometry on rocket performance that are independent of a detailed hydrodynamic analysis. Figure 7 shows reactor weight (assumed to be only that of the moderator) as a function of reactor-cavity radius and length-to-diameter ratio. The upper limits of these curves result from the fact that cavity radii greater than 300 centimeters and/or reactor weights greater than 10^6 pounds are not considered herein.

For a fixed hydrogen flow rate per foot of vortex length, an increase in reactor length results in an increase of both thrust and reactor weight. The solid curves in figure 8 show this geometry effect for cavity length-to-diameter ratios of 1/2, 1, and 2. For a given cavity radius, a length-to-diameter ratio of 2 gives the largest thrust-to-weight ratio. It will be shown subsequently that values of length-to-diameter ratio greater than 2 yield only marginal improvement of performance.

There is, however, another factor to consider here. Since geometry also affects the criticality requirement, the reactor radius and the length-to-diameter ratio cannot be varied independently for a given average fuel density. The dashed lines in figure 8 show how vortex radius and length-to-diameter ratio must be varied in order to maintain a constant critical density. The conclusion to be drawn from the curves of figure 8 is that the more favorable performance will result from a length-to-diameter ratio of 2 and the smallest radius necessary to maintain criticality.

VORTEX HYDRODYNAMIC CHARACTERISTICS

Parameters Considered

For a given set of input flow and geometry parameters the hydrodynamic equations give the radial distribution of the fissionable gas throughout the vortex. This distribution is then used to obtain: (1) average fuel density, (2) reactor size (for a given L/D), and (3) reactor weight. A description of the computer

program format is given in appendix B. The input parameters investigated are as follows: hydrogen flow rate, uranium flow rate, peripheral tangential velocity, vortex-exit-radius ratio, radius ratio of maximum uranium mole fraction x^*, radial Reynolds number (12 for laminar flow, 2.5 for turbulent flow), and radial temperature profile. The input static pressure at x^* is not a primary parameter; it was adjusted in every case to give a pressure at the outer radius of 500 atmospheres.

Effect of Temperature Profile

Two assumed temperature profiles were investigated and are shown in figure 9(a). Both start at 5000° R and increase with decreasing radius to a maximum value of 15,000° R, and of 20,000° R at the center of the vortex. The 20,000° R profiles was used in some of the initial parameter variations, but the "best" performances, both turbulent and laminar, were obtained with the 15,000° R profile.

The effect of the temperature profile on the uranium distribution for a typical laminar flow situation is shown in figure 9(b). The effect is slight and in the expected direction. The lower temperature results in a maximum concentration that is approximately 20/15 higher. The increase of the average concentration in the entire vortex is, of course, considerably less than that of the maximum.

Effect of Hydrogen Flow Rate

Laminar flow. - The effect of hydrogen flow rate on the separation process is shown in figure 10 for laminar flow. The ordinate, the ratio of uranium to hydrogen density, is a measure of how much "separation" has occurred. No separation implies that the uranium streamlines through the vortex are the same as those for hydrogen, and so the density ratio of uranium to hydrogen is constant. This situation occurs for relatively high flow rates. As the hydrogen flow rate is decreased, the amount of separation increases.

Figure 10 illustrates the basic limitation of a single-cavity vortex system where all of the hydrogen must diffuse through the fuel region. The diffusion rates limit the hydrogen flow rates to small values for conditions under which separation will occur. The curves in figure 10 also show why the maximum hydrogen flow rate for a given average uranium density does not necessarily give the maximum thrust per reactor weight. High flow rates give high thrust, but the reactor critical size, and therefore the weight, becomes infinite. For extremely small flow rates, the reactor weight is reasonable, but the thrust is low. This effect is shown in figure 11 for laminar flow and a reactor-cavity length-to-diameter ratio of 2. There is an optimum hydrogen flow rate that gives a maximum reactor thrust-to-weight ratio. For the conditions of this analysis, an optimum will not necessarily occur for all conditions because of the upper limits of 10^6 pounds for reactor weight and 300 centimeters for cavity radius; in such instances the hydrogen flow rate at the cutoff point was used.

Turbulent flow. - The effect of hydrogen flow rate on the separation process is qualitatively the same for turbulent flow as for laminar flow. Figure 12 shows the uranium-to-hydrogen atom-density ratio for three hydrogen flow rates; separation of the uranium occurs for the smaller flow rates.

There is, however, a dissimilarity between laminar and turbulent flow. Although separation does occur for turbulent flow, the actual distribution of uranium in the vortex is such that there is no optimum hydrogen flow rate as shown by the radial uranium distributions in figure 13. In the presence of turbulence, uranium concentrations are much higher near the outer portion of the vortex than for laminar flow. This increase in uranium concentration is a result of the increase of concentration diffusion due to turbulence. Because of this increased concentration and the effect of the radial pressure gradients, a decrease of hydrogen flow rate gives more separation but actually results in lower average fuel density in the reactor. Thus, the "best" performance for turbulent flow is obtained by increasing the propellant flow rate; however, the uranium distribution at high flow rates is such that most of the heat generation, and therefore the high-temperature region, would occur too near the cavity wall. So, the selection of maximum performance for turbulent flow is arbitrary in the sense that it is for a hydrogen flow rate that gives a uranium distribution similar to the curve in figure 13 for 0.0058 pound per second per foot rather than the one for 0.01 pound per second per foot.

Effect of Dissociation

The double maximums exhibited by the uranium-concentration profiles for turbulent flow shown in figure 13 are an interesting result and deserving of comment. The initial increase of uranium concentration near the outer wall indicates that the separation process has started. The decrease in uranium concentration to a minimum at a radius ratio of approximately 0.65 seems to represent a temporary reversal of separation.

The curve for a hydrogen flow rate of 0.0058 pound per second per foot is shown in figure 14 along with hydrogen-species-concentration profiles. The increase in uranium concentration due to the separation process is reversed by the dissociation of molecular hydrogen into atomic hydrogen. After the dissociation process is essentially complete, the separation process again causes an increase in uranium concentration to a second maximum. A similar effect is present for laminar flow but is not significant, because the uranium concentration is much lower where dissociation occurs than for turbulent flow.

Illustrative Laminar Example

The radial variations of the various parameters for a laminar example are illustrated in figure 15. Figure 15(a) shows hydrogen molecular weight, tangential velocity, and static temperature as functions of vortex radius. The static-temperature profile is the same as was shown in figure 9(a), and for laminar flow the tangential velocity varies inversely with the radius. The hydrogen molecular weight is initially at 2 and changes to 1 as dissociation takes place and decreases toward 1/2 as ionization begins. Other hydrogen properties, such as spe-

cific heat, are also taken into account in the program, and these properties are discussed in detail in appendix C.

Figure 15(b) shows the radial velocity variation of hydrogen and uranium. The decrease of the uranium radial velocity at a radius ratio of 0.6 is a measure of the degree of separation; it is essentially the inverse of concentration.

Hydrogen- and uranium-concentration profiles and the static-pressure variation are shown in figure 15(c). The interesting point of this figure is the static-pressure curve. The decrease of static pressure is moderate until the uranium-concentration buildup occurs. The primary decrease in static pressure is due to the presence of the uranium cloud. This is typical of laminar flow where separation is encountered. An excessive static-pressure drop is necessary to diffuse the hydrogen through the fuel-rich region.

ROCKET PERFORMANCE CHARACTERISTICS

Effect of Reactor Length-to-Diameter Ratio

As was shown in figure 8, larger reactor cavity length-to-diameter ratios give higher thrust-to-weight ratios. There is some upper limit at which the assumption of axial independence of the flow field would no longer be valid. It is not necessary to pursue this point, however, because the gain in performance is slight after a length-to-diameter ratio of about 2 is reached as shown in figure 16 for the illustrative laminar example.

The thrust-to-weight ratio goes to 0 at a length-to-diameter ratio equal to zero, because there is no hydrogen flow, but the end moderator-reflector region still gives some reactor weight. At length-to-diameter ratios greater than 2, the increase in critical size causes the reactor weight to increase in proportion to the length.

Effect of Hydrogen-to-Fuel Flow Ratio

A parameter of economic interest, the ratio of hydrogen-to-fuel flow rates, affects the performance through the average fuel density (fig. 17). The decrease in average fuel density with increasing flow-rate ratio is more severe for laminar flow than for turbulent flow. Even for laminar flow, however, this effect is less pronounced than the effect that might be anticipated. A flow-rate ratio of 100 to 1 (the ratio used in the performance optimization) gives average fuel densities that are only 10 percent higher than those that would be obtained for a ratio of 10,000 to 1.

MAXIMUM PERFORMANCE

Fuel Distribution

All the pertinent parameters affecting the separation process were varied to determine their effect on reactor thrust-to-weight ratio. The primary effects

have been shown and discussed. Tangential velocity was limited to 12,600 feet per second at the outer radius; this velocity corresponds to a Mach number of 1.0. Vortex-exit radius ratios and hydrogen flow rates were restricted to combinations within choking limits. The radius ratio of the maximum mole fraction of uranium was varied with the restriction that the uranium-to-hydrogen radial-velocity ratio at the outer radius be a reasonable ($>10^{-2}$) number. This restriction did not actually limit the optimization, since the best performances were for conditions that gave radial-velocity ratios greater than 0.1.

Figure 18 shows the uranium-concentration profiles for the best laminar and turbulent conditions. The performance of turbulent flow could have been improved by about a factor of 2 by increasing the propellant flow rate, but this would have moved the fuel undesirably close to the reactor wall. The curves of figure 18 were obtained for a temperature profile with a 15,000° R maximum value.

Performance Capability

The parameters for the best performance for both laminar and turbulent flows are listed in the following table. For both situations the hydrogen-to-fuel

Parameter	Flow	
	Laminar	Turbulent
Hydrogen-to-fuel flow-rate ratio, w_1/w_2	100	100
Average uranium density, $(B_2)_{av}$, particles/cc	0.46×10^{18}	0.55×10^{18}
Vortex outer radius, r_o, ft	5.5	4.8
Reactor-cavity length-to-diameter ratio, L/D	2	2
Specific impulse, I_{sp}, sec	3000	3000
Thrust, F, lb	530	330
Reactor thrust-to-weight ratio, F/W_R	1.23×10^{-3}	$<1\times10^{-3}$

flow-rate ratio is 100, the reactor cavity length-to-diameter ratio is 2, and the specific impulse is 3000 seconds. The thrust for laminar flow is 530 pounds, and that for turbulent flow is 330 pounds. The maximum thrust-to-weight ratio for laminar flow is 1.2×10^{-3} and for turbulent flow is less than 1×10^{-3}, but just how much less is somewhat arbitrary because it depends on how much uranium can be maintained near the cavity wall. Additional study of this problem is hardly justified, however, since the greatest possible improvement for turbulent flow could

only yield the performance of laminar flow.

To reiterate the conclusion drawn from figure 2, a 3000-second-impulse rocket must have a powerplant thrust-to-weight ratio of at least 10^{-2} to equal the performance of an advanced solid-core system. This ratio is not possible with a single-cavity vortex that requires all of the hydrogen to diffuse through a fuel-rich region. Since all of the assumptions made in the calculation of the performance shown in the table were optimistic, any further effort to determine performance capability more realistically must be considered unnecessary.

ALTERNATE VORTEX SYSTEMS

Any alternate application of a vortex containment scheme to gas-core reactors must provide an increase in thrust of at least two orders of magnitude by either (1) effectively increasing the "length" of the reactor by a multiple tube or a "matrix" arrangement, or (2) flowing only a small (<1 percent) portion of the hydrogen through the fuel region and bypassing the remainder through the cavity in such a way that the energy is acquired by thermal radiation. An analysis of a multiple tube system is given in reference 1, and a vortex matrix is discussed in reference 11.

An illustrative example of a hydrogen bypass flow configuration is shown in figure 19. It should be emphasized that the concept shown is only used to illustrate the principle of bypass flow and does not necessarily represent a feasible arrangement.

A brief calculation was made to determine the possible gain of such a system. The uranium concentration was calculated with the hydrodynamic program for the conditions shown. The hydrogen flow rate necessary to achieve this separation is considerably less than that required to choke the vortex exit. The supplementary hydrogen flow rate was computed from the average vortex-core conditions from the separation program and the choking-limit equation. If the tangential-velocity and static-pressure profiles of the supplementary and primary vortex flows are matched, the two flows may be superimposed with no effect on the vortex strength in the annular region.

If exit choking is the only limit imposed on the supplementary flow, a reactor thrust-to-weight ratio in the range of 1 to 10 appears possible. The heat-transfer mechanism is now primarily thermal radiation rather than molecular collisions. Because the heat source is between the cavity wall and the bypass hydrogen, both the primary hydrogen (to protect the wall) and the supplementary flow would have to be seeded in order to absorb radiant energy. The limit on performance of such a system will be imposed by the amount of radiation reaching the wall and not the separation process. It is possible that such a limit would result in only a marginal increase in performance over that of a reactor with only primary flow.

Again, the system shown in figure 19 is only intended to illustrate the principle of bypass flow as a possible way to increase the performance capabilities of a single-cavity vortex system. Hydrodynamically, the system appears feasible, and the nucleonic characteristics are the same as those investigated

herein. A precise definition of the performance potential of the general system illustrated in figure 19 would require a detailed radiation heat-transfer analysis.

SUMMARY OF RESULTS

An analysis of a single-cavity vortex gaseous reactor was made for dissociating ionizing hydrogen gas and uranium 235 nuclear fuel. To obtain the maximum performance, as measured by reactor thrust-to-weight ratio, optimistic assumptions were made; for example, criticality requirements were used for a reactor cavity with an external moderator of D_2O 100 centimeters thick. An equilibrium specific impulse of 3000 seconds was obtained by (1) the assumption that 10 percent of the total heat generation occurs in the solid region and (2) that hydrogen enters the reactor cavity at 5000° R. The results of this study are summarized as follows:

(1) For laminar flow, the maximum attainable thrust-to-reactor-weight ratio is 1.2×10^{-3}, but for turbulent flow a ratio of less than 10^{-3} is possible.

(2) The low thrust results from the condition that all the hydrogen must diffuse through the fuel-rich region and that a low flow rate is necessary to achieve satisfactory fuel distributions.

(3) For a typical interplanetary mission, a specific impulse of 3000 seconds would require a powerplant thrust-to-weight ratio of 10^{-2} in order to equal the performance of a solid-core nuclear rocket operating at an impulse of 1000 seconds.

(4) For laminar flow, an increase in hydrogen flow rate causes a decrease in average fuel concentration in the reactor; consequently, there is an optimum hydrogen flow rate that gives a maximum thrust-to-weight ratio.

(5) For turbulent flow, an increase of hydrogen flow results in an increase of average fuel concentration because the fuel is moved nearer to the reactor walls; hence, an arbitrary limit on hydrogen flow rate results from wall-heating considerations.

(6) For turbulent flow, the dissociation of hydrogen tends to inhibit the increase of fuel concentration due to the diffusion separation process.

(7) A brief examination of the performance capability of a single-cavity vortex system employing supplementary hydrogen flow through the vortex core indicates that a reactor thrust-to-weight ratio in the range of 1 to 10 may be possible.

CONCLUSIONS

(1) The performance potential of a single-cavity vortex gaseous reactor in which all the propellant must diffuse through the fuel-rich region is less than

that of a solid-core nuclear-rocket engine.

(2) An alternate scheme that offers sufficiently high thrust-to-weight ratios is one which effectively increases the vortex length and, therefore, the propellant flow rate, that is, a vortex "tube bundle" or "matrix" system of many large length-to-diameter ratio parallel vortices. Such systems, however, may incur severe wall-cooling problems that result from greatly reduced thermal radiation path lengths; if so, this would result in a decrease of attainable specific impulse.

(3) A possible application of single-cavity vortex containment to gaseous nuclear rockets is to a system wherein a small fraction, for instance 1 percent, of the total propellant flow passes through the fuel region. The remaining 99 percent of the propellant must then bypass the fuel region and acquire energy by thermal radiation. Such a system is capable of reactor thrust-to-weight ratios of the order of 1 to 10, if it is only limited by the separation process and reactor criticality.

CONCLUDING REMARKS

The primary conclusion reached herein that a single-cavity vortex gaseous reactor where all of the hydrogen must diffuse through the fuel region is inapplicable to rocket propulsion, while perhaps neither surprising nor unique, is based on a consideration of several effects heretofore treated separately. It is expressed or implied, perhaps less specifically, in references 1 and 17, for example. Some previous studies of vortex-reactor schemes have included turbulence effects; others have considered two-component separation in the presence of heat generation, and gas-core nucleonics have also been treated.

A discussion of the effect of hydrogen dissociation and ionization is presented in reference 17 but is not included in the separation analysis. To this author's knowledge, the effect of hydrogen dissociation and ionization on the separation process has not been quantitatively investigated elsewhere. It is included herein with the optimistic assumption that the uranium does not ionize. To this extent, the conclusion presented herein, while unchanged, is on a more comprehensive basis.

The treatment of vortex turbulence in this study follows the general approach of previous work reported in references 2, 3, 7, 8, 9, 10, and 11. Here the deviations of tangential-velocity and static-pressure profiles from laminar theory predictions are attributed to the presence of an axially independent turbulent flow field. This procedure appears valid, at least to the extent that it has been used to correlate existing vortex data for single-component compressible flow. Recent studies (e.g., ref. 20) indicate that at least part of the indicated deviation from two-dimensional laminar flow results from boundary-layer effects on the end surfaces of a confined vortex. Such an approach suggests that vortex turbulence levels may be less than anticipated. Since a quantitatively usable understanding of all of the factors governing single-component vortex flow is not presently available, a more elaborate treatment of a two-component vortex than that used in this report is not warranted at this time.

In order to obtain a maximum performance capability, it was not necessary to consider in detail the effect of uranium-to-hydrogen radial-velocity ratio at the point of injection, $(u_2/u_1)_o$, on the separation process. The best performance was determined by a free choice of the radius ratio at which the fuel concentration is a maximum. This choice then determines a value of $(u_2/u_1)_o$ - a value that might not be physically attainable. So, while the maximum performance is readily calculable, a determination of the most probable performance would require an additional consideration of what boundary values of $(u_2/u_1)_o$ are possible in a two-component vortex system.

A few comments about a bypass flow vortex system are appropriate. Consider a single-cavity vortex with a sufficiently low flow rate of primary hydrogen diffusing through the fuel region that a critical concentration exists. If a small (i.e., 10 percent of the primary flow) amount of supplementary hydrogen, seeded so as to be opaque, is introduced into the core of the vortex, it will be heated by thermal radiation to a temperature that is effectively that of the exhausting primary flow. Thus some improvement in performance seems possible.

In order to obtain thrust-to-weight levels of interest, however, a supplementary flow at least ten times that of the primary flow would be required. The fuel-region temperature would have to be increased in order to radiatively heat the supplementary flow to a sufficiently high temperature, which, in turn, would increase the radiation heat transfer to the reactor wall. It therefore appears that an optimum supplementary flow rate would exist in terms of an increased thrust-to-weight ratio and a decreased specific impulse. The maximum possible thrust-to-weight ratio (1 to 10) of a supplementary flow system is high enough to warrant a more detailed analysis of the limits imposed by thermal radiation.

Lewis Research Center
National Aeronautics and Space Administration
Cleveland, Ohio, November 16, 1962

APPENDIX A

SYMBOLS

A	area, sq ft
$a_1, \ldots, a_5$	numerical constants for temperature profile
B	density, particles/cc
b	constant in diffusion equation
C	parameter in velocity profile
c_p	specific heat, Btu/(lb)(^oF)
D	reactor-cavity diameter, ft
D_{12}	binary diffusion coefficient, sq ft/sec
F	thrust, lb force
g	gravitational constant, ft/sec^2
I_{sp}	specific impulse, sec
J	mechanical equivalent of heat, ft-lb/Btu
L	reactor-cavity length, ft
M	molecular weight, lb/(lb)(mole)
n	molar density, (lb)(mole)/cu ft
P	total pressure, lb/sq ft
p	static pressure, lb/sq ft
R	universal gas constant, ft-lb/(lb)(mole)(^oR)
Re	radial Reynolds number
r	radius, ft, except as indicated
T	total temperature, ^oR
t	static temperature, ^oR
u	radial velocity, ft/sec
V_i	molecular volume of species i, cc/(g)(mole)

v tangential velocity, ft/sec

W weight, lb

w mass flow rate per reactor length, lb/(sec)(ft)

x vortex radius ratio, r/r_o

y mole fraction

z axial coordinate, ft

α_2 parameter in diffusion equation, sq ft

β parameter in diffusion equation, sq ft

γ ratio of specific heats

ϵ eddy diffusivity, sq ft/sec

θ angular coordinate, radians

μ viscosity, lb/(ft)(sec)

ρ density, lb/cu ft

φ percent of total power

ψ function in velocity profile (see eq. (11))

Subscripts:

av average

c critical

ch choking

l laminar

ma mass

mo momentum

n vortex inner radius

o vortex outer radius

R reactor

s sonic

t turbulent

1 hydrogen

2 uranium

Superscripts:

' normalized to value at $\bar{r}_n$

* indicates radial position of maximum y_2

APPENDIX B

COMPUTER PROGRAM

By Muriel B. Eian

At the end of this appendix is a listing of the vortex gaseous-reactor hydrodynamic code written in Fortran for the IBM 7090 digital computer operating with the Lewis monitor system. Basically, it is a solution of two first-order nonlinear equations (diffusion and momentum for a two-component vortex field) using the Runge-Kutta numerical technique to compute uranium mole fraction and static pressure as a function of radial position. A block diagram of the program is given in figure 20.

The code can be run for either laminar or turbulent flow ("computed go to" controlled). Computation is initiated at an assigned (input) starting radius ratio x^*, where dy_2/dx is set equal to zero and pressure p is set equal to some starting value PRE. The program calculates hydrodynamic parameters from x^* to $x = 1$. The calculation returns to x^* and then proceeds to x_n. At this point, vortex-core equations are substituted for annular equations, and the calculation proceeds inward to some arbitrary terminal radius x_s.

Calculations can be made for either adiabatic or heat-generation (sense-switch controlled) conditions.

When heat is generated, subroutine curve fit (SUB CF) is called. This subroutine is based on an arbitrary temperature-distribution curve of temperature t against radius x. At each value of x, the static temperature is determined from a five-coefficient polynomial in the form of $t = a_1 + a_2x + a_3x^2 + a_4x^3 + a_5x^4$, where the coefficients are input to the program in the following form:

$$(a_1, a_2, a_3, a_4, a_5)_1 \qquad 1 \geq x > 0.725$$

$$(a_1, a_2, a_3, a_4, a_5)_2 \qquad 0.725 \geq x > 0.65$$

$$(a_1, a_2, a_3, a_4, a_5)_3 \qquad 0.65 \geq x > 0.55$$

$$(a_1, a_2, a_3, a_4, a_5)_4 \qquad 0.55 \geq x > 0$$

Choices of the previous Δx's are arbitrary and can be varied to fit the curve.

At each value of x, subroutines SUB INT and SUB YH are called. In SUB INT static pressure and static temperature are used to determine hydrogen properties (described in appendix C). In SUB YH the hydrogen properties are used to calculate hydrogen molecular weight, specific-heat ratio, mole fraction of H, mole

fraction of H_2, and mole fraction of H^+.

When heat is not generated, static temperature, static-temperature ratio, total temperature, and total-temperature ratio are computed from adiabatic-flow equations using input values for specific heat, specific-heat ratio, and hydrogen molecular weight.

An initial increment size of $\Delta x = 0.0005$ is used to start the calculation. At each subsequent step, the increment size is adjusted according to the test:

$\lvert dy_2/dx \rvert$	Δx
0 - 1	0.0005
1 - 10	0.0001
10 - ∞	0.00005

The output is keyed to a counter and increment size so that it occurs at Δx intervals of 0.05.

Accuracy of this problem that uses the Runge-Kutta numerical technique is dependent on the size of the increment. Sizes of increments were decreased and problems were run until no significant difference in y_2 was noted.

For a typical laminar example, doubling Δx resulted in less than 0.1 of 1 percent change in y_2 near the peak.

INPUT

The program input is required in the following order:

(1) *Data

(2) Binary deck. Table of hydrogen properties (CP, ALPHA, BETA), at 40 values of temperature for each of 10 pressure levels. (This deck is read in once with main deck.)

(3) Card number 1 Format (I4)
Control words - The "computed go to" words necessary to specify which case is to be run are: (1) laminar, (2) turbulent.

(4) Card number 2
Sense switch control words are used as follows: Sense switch (1) controls adiabatic (on) or heat generation (off). Sense switch (2) controls computation of eddy diffusivity. Static pressure and temperature ratios are set to 1.0 (on).

(5) Card number 3 Format (7F10.5)

W1L hydrogen flow rate, lb/(sec)(ft)

W2L uranium flow rate, lb/(sec)(ft)

XSTAR starting radius ratio ($dy_2/dx = 0$)

REMO Reynolds number for momentum transfer

AM2 uranium molecular weight

VO tangential velocity at $x = 1.0$, ft/sec

TO static temperature at $x = 1.0$ (for no heat generation)

(6) Card number 4 Format (7F10.5)

PRE starting pressure, atm

XN vortex-exit radius ratio

REMA Reynolds number for mass transfer

VIN molecular volume term in Gilliland equation

S constant for Newton test

RUN run number

CPA specific heat (for no heat generation)

(7) Card number 5 Format (7F10.5)

AMI hydrogen molecular weight (for no heat generation)

GAMMA specific-heat ratio (for no heat generation)

(8) Cards 6 to 10 Format (4E15.8)
Constants for curve fit routine

(9) Card number 11 Format (7F10.5,315)

DELT 1, DELT 2, DELT 3 } increment step size

XS terminal radius

N1, N2, N3 } constants for output counter

W1L hydrogen flow rate, lb/(sec)(ft)

W2L uranium flow rate, lb/(sec)(ft)

XSTAR starting radius ratio ($dy_2/dx = 0$)

REMO Reynolds number for momentum transfer

AM2 uranium molecular weight

VO tangential velocity at x = 1.0, ft/sec

TO static temperature at x = 1.0 (for no heat generation)

(6) Card number 4 Format (7F10.5)

PRE starting pressure, atm

XN vortex-exit radius ratio

REMA Reynolds number for mass transfer

VIN molecular volume term in Gilliland equation

S constant for Newton test

RUN run number

CPA specific heat (for no heat generation)

(7) Card number 5 Format (7F10.5)

AMI hydrogen molecular weight (for no heat generation)

GAMMA specific-heat ratio (for no heat generation)

(8) Cards 6 to 10 Format (4E15.8)
Constants for curve fit routine

(9) Card number 11 Format (7F10.5,3I5)

DELT 1, DELT 2, DELT 3 } increment step size

XS terminal radius

N1, N2, N3 } constants for output counter

OUTPUT

Input parameters, type of calculation, and starting values at x^* are the initial output. Then pertinent parameters are read out at intervals of approximately 0.05 in x.

RUNNING TIME

Program running time is somewhat dependent on the input, since Δx is adjusted as a function of dy_2/dx; for heat-generation runs the average running time on the IBM 7090 with the Lewis monitor system is approximately 3 minutes. The no-heat-generation runs, because hydrogen-property interpretations are not required, have a running time of about 2 minutes.

```
      DIMENSION T(10,40),CP(10,40),ALPHA(10,40),BETA(10,40),P(10)
      DIMENSION AT(40),ACP(40),ALP(40),BET(40),PPP(4),TEMP1(4)
      DIMENSION TEMP2(4),TEMP3(4)
      COMMON T,CP,ALPHA,BETA,P,AT,ACP,ALP,BET,PPP,TEMP1,TEMP2,TEMP3,PP,T
     1T,ANS1,ANS2,ANS3,YH2,YH,YHPLUS,GAMMA,AM1,X,  ZA,ZB,ZC,ZD,ZE,YA,YB,
     2YC,YD,YE,XA,XB,XC,XD,XE,WA,WB,WC,WD,WE,XSQ,X3,X4,TLIL
      CALL BC READ(T(10,40),T(1,1))
      CALL BC READ(CP(10,40),CP(1,1))
      CALL BC READ(ALPHA(10,40),ALPHA(1,1))
      CALL BC READ(BETA(10,40),BETA(1,1))
      CALL BC READ(P(10),P(1))
    3 FORMAT(4F10.5,3I5)
    4 FORMAT(1H0E15.8,6E17.8)
    6 FORMAT(1H0,9X,2HCP,13X,5HALPHA,11X,4HBETA,12X,4HTEMP,13X,4HPRES)
    7 FORMAT(E15.8,6E17.8)
    8 FORMAT(E15.8,E17.8,E16.8,E17.8,E16.8,E17.8,E16.8,F6.0)
    9 FORMAT(7F10.5)
   10 FORMAT(4E15.8)
   33 FORMAT(21H0 PRESSURE OVER 1000.)
   39 FORMAT(1H0,7X,2HM1,13X,5HGAMMA,12X,2HYH,14X,3HYH2,13X,6HYHPLUS,13X
     1,2HCP)
   40 FORMAT(1H0E25.8,E29.8,E28.8,E16.8,E16.8)
   41 FORMAT(106H0                    X                                  Y2
     1                  U2/U1          B2                 C2)
   42 FORMAT(1H0,8X,1HV,12X,6HTS/TS*,12X,2HB1,14X,2HC1,12X,6HTT/TT*,10X,
     16HPS/PS*,10X,6HPT/PT*,11X)
   43 FORMAT(20H0 NO HEAT GENERATION)
   44 FORMAT(17H0 HEAT GENERATION)
   45 FORMAT(16H0TLIL MINUS STOP)
   46 FORMAT(16H0U2U1 MINUS STOP)
   47 FORMAT(16H0 Y2  MINUS STOP)
   48 FORMAT(18H0 Y2 OVER ONE STOP)
   49 FORMAT(E15.8,7E16.8)
   71 FORMAT(1H0,7X,1HV,13X,6HTS/TS*,12X,2HB1,14X,2HC1,10X,6H  TEMP,12X,
     16H  PRES)
   95 FORMAT(I4)
   97 FORMAT(62H1                                                    TURBULENT P
     1ROGRAM)
   98 FORMAT(62H1                                                     LAMINAR P
     1ROGRAM)
   99 FORMAT(102H0                          PEAK-TO-WALL CALCULATIONS FOR
     1VORTEX CAVITY REACTOR   RAGSDALE-EIAN  PAX 2115)
  106 FORMAT(118H0    W1L              W2L              XSTAR
     1 REMO           AM1              AM2              V0          RUN)
  107 FORMAT(120H0    PSI1             PSI2             PSI20
     1 TLILS            TBIGS             BP                 DN         )
  108 FORMAT(120H0    ALPH2            Y2STA             U2U1S
     1  PS*                                                             )
  109 FORMAT(62H0     REMA             XM
     1      )
      PI=3.14159
      G=32.2
      AJ=778.0
      RG=1544.0
   22 READ INPUT TAPE 7,95,IG
      GO TO (208,207,207),IG
  208 WRITE OUTPUT TAPE 6,98
      WRITE OUTPUT TAPE 6,99
      GO TO 2
  207 WRITE OUTPUT TAPE 6,97
```

```
      WRITE OUTPUT TAPE 6,99
    2 CALL READ SS
      READ INPUT TAPE 7,9,W1L,W2L,XSTAR,REMO,AM2,V0,T0,PRE,XN,REMA,VIN,S
     1,RUN,CPA,AM1,GAMMA
      READ INPUT TAPE 7,10,ZA,ZB,ZC,ZD,ZE,YA,YB,YC,YD,YE,XA,XB,XC,XD,XE,
     1WA,WB,WC,WD,WE
      READ INPUT TAPE 7,3,DELT1,DELT2,DELT3,XS,N1,N2,N3
  111 KTR=0
      RE=REMO
      C=(1./(2.-RE))*(RE/(EXPF(RE/2.)-1.))
      VOROP=1.0+C*(XN**(RE-2.)-1.)
      TEM=(1.0/VOROP)**2
      TEM1=(1.0-C)**2
      TEM2=C-C*C
      TEM3=(XSTAR/XN)
      TEM4=TEM3**(RE-2.)
      TEM5=TEM3**(2.*RE-4.)
      TEM6=TEM2/TEM4
      TEM7=C*C/TEM5
      TEM88=TEM1+2.*TEM6+TEM7
      PSI1=TEM88*TEM
      V=(V0*SQRTF(PSI1))/XSTAR
      TEM89=TEM1*(1.-4./RE)-(4./RE*TEM6)-TEM7
      PSI2=TEM89*TEM
      XSQST=XSTAR*XSTAR
      X3ST=XSTAR*XSQST
      X=XSTAR
      XSQ=XSQST
      X3=X*XSQ
      X4=XSQ*XSQ
      TEM 90=2.*CPA*G*AJ
      TEM91=V0*V0
      IF(SENSW(1))503,504,504
  503 PSI20=TEM*(TEM1*(1.-4./RE)-((4./RE)*(TEM2/(1./XN)**(RE-2.)))-(C*C/
     1(1./XN)**(2.*RE-4.)))
      WRITE OUTPUT TAPE 6,43
      TINFI=T0+PSI20*TEM91/TEM90
      TLILS=TINFI-(PSI2*TEM91/(TEM90*XSQST))
      IF(TLILS)50,51,51
   50 WRITE OUTPUT TAPE 6,45
      GO TO 22
   51 TBIGS=TLILS+V*V/TEM90
      GO TO 513
  504 CALL CF
      TT=TLIL
      PP=PRE
      TLILS=TLIL
      CALL INT
      WRITE OUTPUT TAPE 6,6
      WRITE OUTPUT TAPE 6,7,ANS1,ANS2,ANS3,TT,PP
      TEM 90=2.*ANS1*G*AJ
      TBIGS=TLILS+V*V/TEM90
      WRITE OUTPUT TAPE 6,44
      CALL SUB YH
  513 TEM92=G*RG*TLILS
      BP=(AM2-AM1)*TEM91*PSI1/TEM92
      DN=(2.62E-6*SQRTF((1./AM1+1./AM2)*TLILS))/VIN
      CON8=W1L/W2L*(AM2/AM1)
      B=1.0+CON8
      CON=W1L+W2L
      CON1=2.*PI*REMA
```

```
      TL2=DN
      ALPH2=W2L/(2.*PI*AM2*TL2)
      CON5=ALPH2*XSQST/BP
      CON6=CON5*B-1.0
      CON7=SQRTF(CON6*CON6+(4.*CON5))
      Y2STA=((-CON6   )+CON7)/2.0
  407 FY=(-ALPH2*(B*Y2STA-1.0)/XSTAR)+(BP*(Y2STA-Y2STA*Y2STA)/X3ST)
      IF(ABSF(FY)-(S*Y2STA))405,405,406
  406 FPY=((-ALPH2*B)/XSTAR)+(BP/X3ST)-((2.0*BP/X3ST)*Y2STA)
      DY2=FY/FPY
      Y2STA=Y2STA-DY2
      GO TO 407
  405 U2U1S=((1./Y2STA)-1.)/CON8
      P0PST=1.0
      P0P0=P0PST
      X=XSTAR
      Y2=Y2STA
      Y1=1.0-Y2STA
      TEM15=GAMMA/(GAMMA-1.0)
      TEM16=XSQST*GAMMA*TEM92
      TEM17=(GAMMA-1.0)/2.0
      TEM18=(TEM91*PSI1*(Y1*AM1+Y2*AM2))/TEM16
      P4S=P0P0*(1.0+TEM17*TEM18)**TEM15
      PP=PRE
      WRITE OUTPUT TAPE 6,106
      WRITE OUTPUT TAPE 6,8,W1L,W2L,XSTAR,REMO,AM1,AM2,V0,RUN
      WRITE OUTPUT TAPE 6,109
      WRITE OUTPUT TAPE 6,7,REMA,XN
      WRITE OUTPUT TAPE 6,107
      WRITE OUTPUT TAPE 6,7,PSI1,PSI2,PSI20,TLILS,TBIGS,BP,DN
      WRITE OUTPUT TAPE 6,108
      WRITE OUTPUT TAPE 6,7,ALPH2,Y2STA,U2U1S,PRE
      WRITE OUTPUT TAPE 6,41
      IF(SENSW(1))64,63,63
   64 WRITE OUTPUT TAPE 6,42
      GO TO 12
   63 WRITE OUTPUT TAPE 6,71
      WRITE OUTPUT TAPE 6,39
   12 TEM3=X/XN
      TEM4=TEM3**(RE-2.)
      TEM5=TEM3**(2.*RE-4.)
      TEM6=TEM2/TEM4
      TEM7=C*C/TEM5
      TEM88=TEM1+2.*TEM6+TEM7
      PSI1=TEM88*TEM
      V=(V0*SQRTF(PSI1))/X
      TEM89=TEM1*(1.-4./RE)-(4./RE*TEM6)-TEM7
      PSI2=TEM89*TEM
      XSQ=X*X
      IF(X-1.0000001)525,525,22
  525 IF(SENSW(1))515,516,516
  515 TLIL=TINFI-(PSI2*TEM91/(TEM90*XSQ))
      TTLIL=TLIL/TLILS
      TBIG=TLIL+V*V/TEM90
      TTBIG=TBIG/TBIGS
      GO TO 517
  516 X3=XSQ*X
      X4=XSQ*XSQ
      CALL CF
      TT=TLIL
```

```
    TEM 90=2.*ANS1*G*AJ
    TBIG=TLIL+V*V/TEM90
    TTLIL=TLIL/TLILS
    TTBIG=TBIG/TBIGS
    IF(TLIL)50,517,517
517 TEM92=G*RG*TLIL
    P10P0=Y1*P0P0
    P20P0=Y2*P0P0
    IF(SENSW(1))66,67,67
 67 CALL INT
    IF(PP-1000.)83,83,84
 84 WRITE OUTPUT TAPE 6,33
    GO TO 22
 83 CALL SUB YH
 66 BP=(AM2-AM1)*TEM91*PSI1/TEM92
    DN=(2.62E-6*SQRTF((1./AM1+1./AM2)*TLIL))/VIN
    C1=2.22E-3*RG*TLIL*W1L /(2.*X*AM1*P10P0)*PRE*14.7
    C2=2.22E-3*RG*TLIL*W2L /(2.*X*AM2*P20P0)*PRE*14.7
    B1=(1.385E+24*P10P0)/(RG*TLIL)*PRE*14.7
    B2=(1.385E+24*P20P0)/(RG*TLIL)*PRE*14.7
    TEM 15=GAMMA/(GAMMA-1.0)
    TEM16=X*X*GAMMA*G*RG*TLIL
    TEM17=(GAMMA-1.0)/2.0
    TEM18=(TEM91*PSI1*(Y1*AM1+Y2*AM2))/TEM16
    P4=P0P0*(1.0+TEM17*TEM18)**TEM15
    PPBIG=P4/P4S
    CON8=W1L/W2L*(AM2/AM1)
    U2U1=((1./Y2)-1.0)/CON8
 54 GO TO(526,527,527),IG
527 TL2=DN
    IF (SENSW(2))634,635,635
634 P0PST=1.0
    TST0T=1.0
    CON6=2.*PI*REMA
    EN=(CON*P0PST*TST0T)/(CON6*(Y2*AM2+Y1*AM1))
    GO TO 530
635 CON6=2.*PI*REMA
    CON9=TLILS/TLIL
    EN=(CON*P0P0*CON9)/(CON6*(Y2*AM2+Y1*AM1))
    GO TO 530
526 TL2=DN
530 ALPH2=W2L/(2.*PI*AM2*TL2)
    GO TO (532,533,533),IG
532 TEM8=1.0
    GO TO 52
533 TEM8=DN/(DN+EN)
 52 DYDX =(((Y2-Y2*Y2)*BP/X**3)-((B*Y2-1.0)*ALPH2/X))*TEM8
    Y2P=SQRTF(DYDX*DYDX)
    IF(Y2P-1.0)13,13,14
 13 DELTX=DELT1
    N=N1
    GO TO 17
 14 IF(Y2P-10.)15,15,16
 15 DELTX=DELT2
    N=N2
    GO TO 17
 16 DELTX=DELT3
    N=N3
 17 IF (XMODF(KTR,N))18,19,18
 19 KTR=KTR+1
    WRITE OUTPUT TAPE 6,40,X,Y2,U2U1,B2,C2
```

```
    IF (SENSW(1))80,81,81
81  WRITE OUTPUT TAPE 6,7,V,TTLIL,B1,C1,TT,PP
    WRITE OUTPUT TAPE 6,4,AM1,GAMMA,YH,YH2,YHPLUS,ANS1
    GO TO 20
80  WRITE OUTPUT TAPE 6,49,V,TTLIL,B1,C1,TTBIG,PP,PPBIG
    GO TO 20
18  KTR=KTR+1
20  V02=TEM91
    TEM13=G*RG*TLIL
    AAK1=TEM8*(-ALPH2*(B*Y2-1.0)/X+BP*(Y2-(Y2*Y2))/X**3)*DELTX
    AAL1=(((1.-Y2)*AM1+Y2*AM2)*V02*PSI1*P0P0*DELTX)/(TEM13*X**3)
    TEM9=X+(DELTX/2.0)
    TEM10=TEM9**3
    TEM11=Y2+(AAK1/2.0)
    AAK2=TEM8*((-ALPH2*(B*TEM11-1.0)/TEM9)+(BP*(TEM11-TEM11*TEM11)/TEM
   110))*DELTX
    TEM12=Y2+(AAK2/2.0)
    AAL2=(((1.-TEM11)*AM1+TEM11*AM2)*V02*PSI1*(P0P0+AAL1/2.0)*DELTX)/(
   1TEM13*TEM10)
    TEM15=X+DELTX
    AAK3=TEM8*(-ALPH2*(B*TEM12-1.0)/TEM9+BP*(TEM12-TEM12*TEM12)/TEM10)
   1*DELTX
    TEM14=Y2  +AAK3
    AAL3=((1.-TEM12)*AM1+TEM12*AM2)*V02*PSI1*(P0P0+AAL2/2.0)*DELTX/(TE
   1M13*TEM10)
    AAL4=((1.0-Y2+AAK3)*AM1+AM2*(Y2+AAK3))*V02*PSI1*(P0P0+AAL3)*DEL
   1TX/(TEM13*(X  +DELTX)**3)
    AAK4=TEM8*( -ALPH2*(B*TEM14 -1.0)/TEM15+BP*(TEM14-TEM14*TEM14)/TE
   1M15**3)*DELTX
    DELTY2=(AAK1+2.0*AAK2+2.0*AAK3+AAK4)/6.0
    DP0P0=(AAL1+2.0*AAL2+2.0*AAL3+AAL4)/6.0
    Y2=DELTY2+Y2
    IF(Y2)55,56,56
55  Y2=0
56  IF(Y2-1.0000001)57,57,58
58  WRITE OUTPUT TAPE 6,48
    GO TO 22
57  Y1=1.0-Y2
    P0P0=DP0P0+P0P0
    IF (SENSW(1))73,74,74
73  PP=P0P0
    GO TO 76
74  PP=P0P0*PRE
76  X=X+DELTX
    IF(X-1.0000001)59,59,60
59  GO TO 12
60  GO TO 22
    END
```

APPENDIX C

HYDROGEN PROPERTIES

Hydrogen properties used in this study were computed from results presented in reference 19. The properties of interest herein are (1) equilibrium species mole fraction of H_2, H, and H^+; (2) specific heat at constant pressure; (3) ratio of specific heats; and (4) average hydrogen molecular weight. The symbols used in this appendix are defined in the following paragraph and, where applicable, are the same as in reference 19.

For a range of temperatures ($^\circ K$) and pressures (atm), reference 19 gives a tabular listing of α, β, and H/M, where H/M is enthalpy in calories per gram. For N initial atoms of H, the equilibrium species concentrations are, by definition:

$\alpha N/2$	H_2 molecules
βN	H^+ protons
βN	electrons
$(1 - \alpha - \beta)$	H atoms

From these parameters of reference 19, the values used herein were computed from the following equations:

$$y_{H_2} = \frac{\alpha}{2 + 2\beta - \alpha}$$

$$y_H = \frac{1 - \alpha - \beta}{1 + \beta - (\alpha/2)}$$

$$y_{H^+} = \frac{\beta}{1 + \beta - (\alpha/2)}$$

$$M_{av} = 2.016\, y_{H_2} + 1.008(y_H + y_{H^+})$$

$$c_p = \left[\frac{\partial(H/M)}{\partial t}\right]_p \cong \frac{(H/M)_{t,1} - (H/M)_{t,2}}{t_1 - t_2}$$

where c_p is at a temperature equal to $(t_1 + t_2)/2$

$$\gamma \equiv \frac{c_p}{c_v} = \frac{Jc_pM_{av}/R}{(Jc_pM_{av}/R) - 1}$$

The input to the hydrodynamic program properties subroutine was in the form of tables. There were ten tables, one for each of the following pressures: 10^{-5}, 10^{-4}, 10^{-3}, 10^{-2}, 10^{-1}, 1, 10, 100, 300, and 500 atmospheres. For each pressure, values of α, β, and c_p were listed for 40 temperatures ranging from 900° to 39,600° R. A five-point two-variable Lagrange interpolation procedure was used to obtain values of α, β, and c_p for any desired pressure and temperature conditions in the vortex.

The output of this subroutine is shown in figure 21 for pressures of 1, 100, and 500 atmospheres and for temperatures from 5000° to 22,000° R. Figure 21(b), the average hydrogen molecular weight, represents the most significant effect of dissociation and ionization of the propellant on the separation. The computed average molecular weight affects both the binary diffusion coefficient and the static-pressure gradient of the hydrogen in the vortex. Equilibrium specific heat is of considerable importance, of course, but for the arbitrary temperature profile employed in the hydrodynamic program this effect is hidden.

REFERENCES

1. Kerrebrock, Jack L., and Meghreblian, Robert V.: Vortex Containment for the Gaseous-Fission Rocket. Tech. Release 34-205, Jet Prop. Lab., C.I.T., Sept. 1961. (See also Jour. Aero/Space Sci., vol. 28, no. 9, Sept. 1961, pp. 710-724.)

2. Ragsdale, Robert G.: NASA Research on the Hydrodynamics of the Gaseous Vortex Reactor. NASA TN D-288, 1960.

3. Keyes, J. J., Jr., and Dial, R. E.: An Experimental Study of Vortex Flow for Application to Gas-Phase Fission Heating. ORNL 2837, Oak Ridge Nat. Lab., Apr. 16, 1960.

4. Meghreblian, Robert V.: Performance Potential of Nuclear Rockets. Tech. Release 34-96, Jet Prop. Lab., C.I.T., July 6, 1960.

5. Meghreblian, Robert V.: Gaseous Fission Reactors for Spacecraft Propulsion. Tech. Rep. 32-42, Jet Prop. Lab., C.I.T., July 6, 1960.

6. Meghreblian, Robert V.: Prospects for Advanced Nuclear Systems. Tech. Memo. 33-40, Jet Prop. Lab., C.I.T., Mar. 8, 1961.

7. Ragsdale, Robert G.: Applicability of Mixing Length Theory to a Turbulent Vortex System. NASA TN D-1051, 1961.

8. Donaldson, Coleman duP.: The Magnetohydrodynamic Vortex Power Generator - Basic Principles and Practical Problems. Rep. 30, Aero. Res. Associates of Princeton, Inc., Mar. 1961.

9. Williamson, Guy G., and McCune, James E.: A Preliminary Study of the Structure of Turbulent Vortices. Rep. 32, Aero. Res. Associates of Princeton, Inc., July 1961.

10. Deissler, R. G., and Perlmutter, M.: Analysis of the Flow and Energy Separation in a Turbulent Vortex. Int. Jour. Heat Mass Transfer, vol. 1, Pergamon Press, 1960, pp. 173-191.

11. Rosenzweig, Martin L., Lewellen, W. S., and Kerrebrock, Jack L.: The Feasibility of Turbulent Vortex Containment in the Gaseous Fission Rocket. Preprint 1516A-60, Am. Rocket Soc., Inc., 1960.

12. Meghreblian, Robert V.: Thermal Radiation in Gaseous Fission Reactors for Propulsion. Tech. Rep. 32-139, Jet Prop. Lab., C.I.T., July 24, 1961.

13. Spencer, D. F.: Thermal and Criticality Analysis of the Plasma Core Reactor. Tech. Rep. 32-189, Jet Prop. Lab., C.I.T., Jan. 1, 1962.

14. Wahl, B. W., Gould, R. J., and McKee, J. W.: Radiative Properties of Hydrogen and Radiative Transfer to the Environment at Elevated Temperatures. Eng. Paper 1149, Douglas Aircraft Co., Inc., Aug. 1961.

15. Hyland, Robert E., Ragsdale, Robert G., and Gunn, Eugene J.: Two-Dimensional Criticality Calculations of Gaseous-Core Cylindrical Cavity Reactors. NASA TN D-1575, 1962.

16. Hallet, R. W., Jr., McKee, J. W., and Faller, R. J.: Operational Use of Gas Core Nuclear Reactors Propulsion Systems in Large, Manned, High-Thrust Spacecraft. Eng. Paper 1200, Douglas Aircraft Co., Inc., Sept. 1961.

17. McLafferty, George H.: Theoretical Analysis of Multi-Unit Rotating-Gaseous-Core Nuclear Rockets. Rep. R-1686-3, United Aircraft Corp., Apr. 1960.

18. Himmel, S. C., et al.: Nuclear-Rocket Vehicles for Mars and Venus Missions. Paper presented at ARS/ORNL Space-Nuclear Conf., Gatlinburg (Tenn.), May 3-5, 1961.

19. Rosenbaum, Burt M., and Levitt, Leo: Thermodynamic Properties of Hydrogen from Room Temperature to 100,000° K. NASA TN D-1107, 1962.

20. Kendall, James M., Jr.: Experimental Study of a Compressible Viscous Vortex. Tech. Rep. 32-290, Jet Prop. Lab., C.I.T., June 1962.

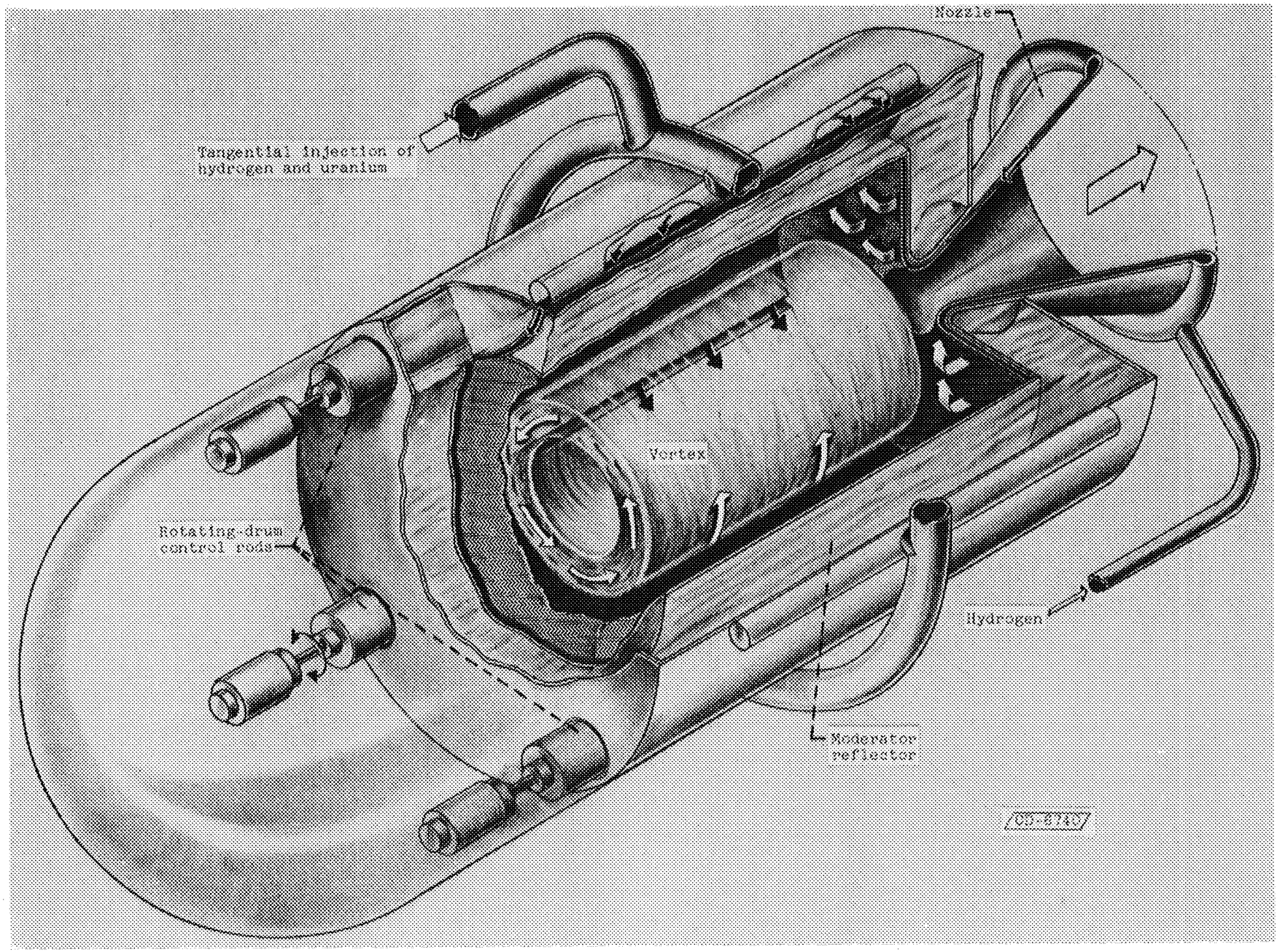

Figure 1. - Single-cavity vortex gaseous nuclear reactor showing general flow pattern.

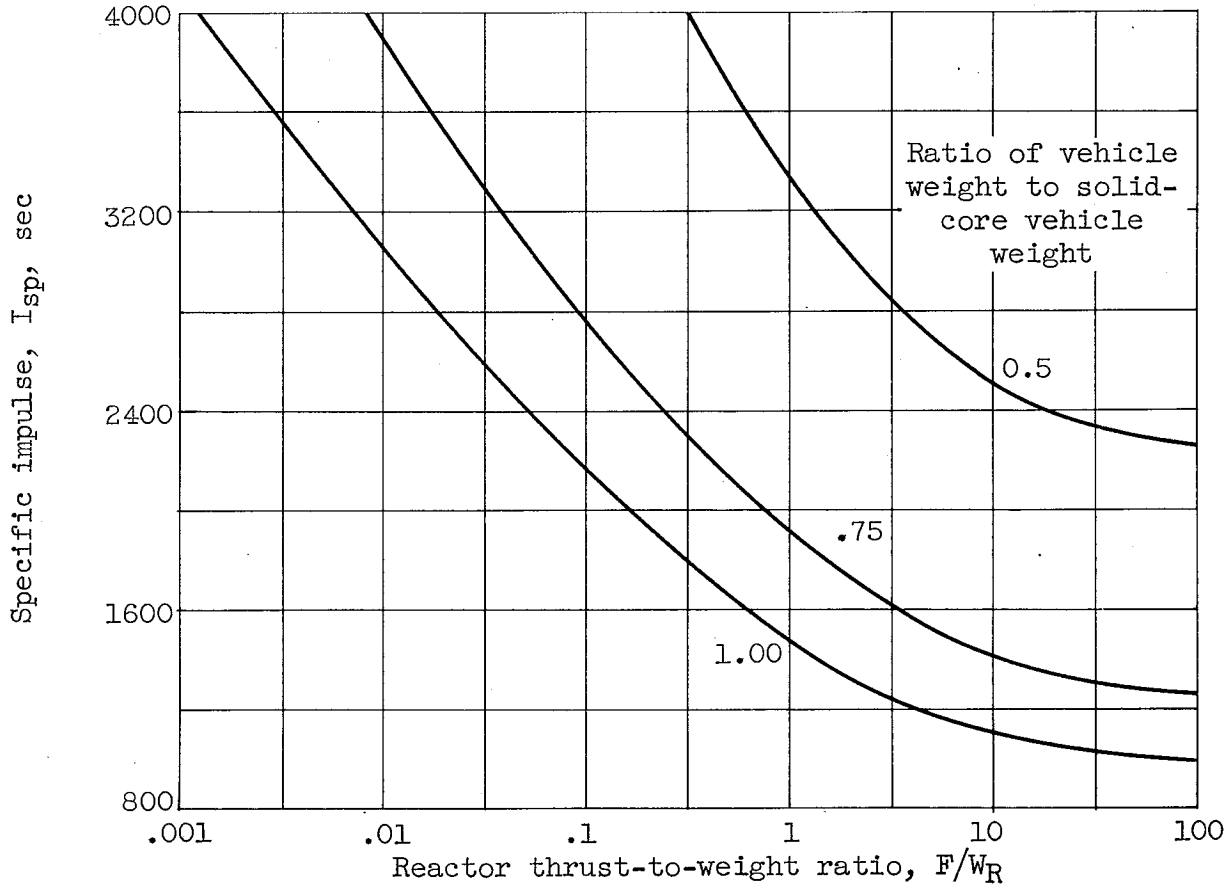

Figure 2. - Effect of reactor thrust-to-weight ratio on specific impulse requirement for seven-man 460-day Venus mission.

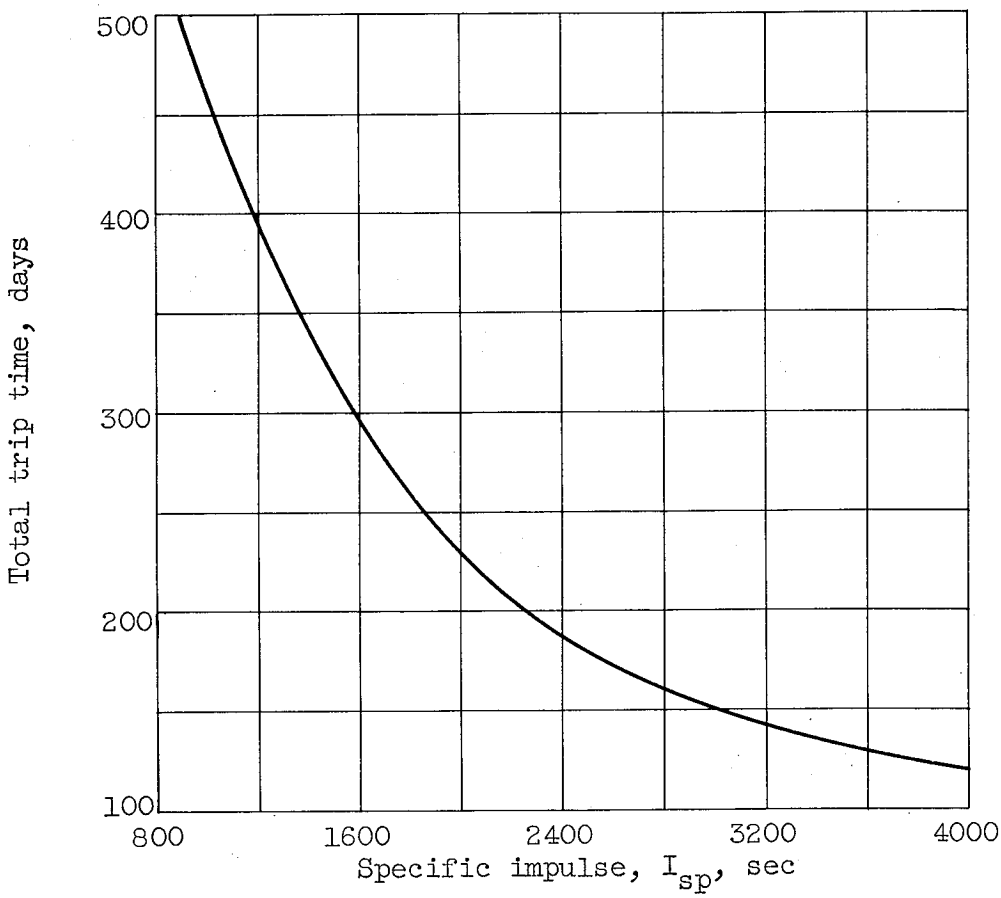

Figure 3. - Effect of specific impulse on mission time for seven-man Venus mission. Initial weight in orbit, 1.7×10^6 pounds; thrust per reactor weight, $>10^{-1}$.

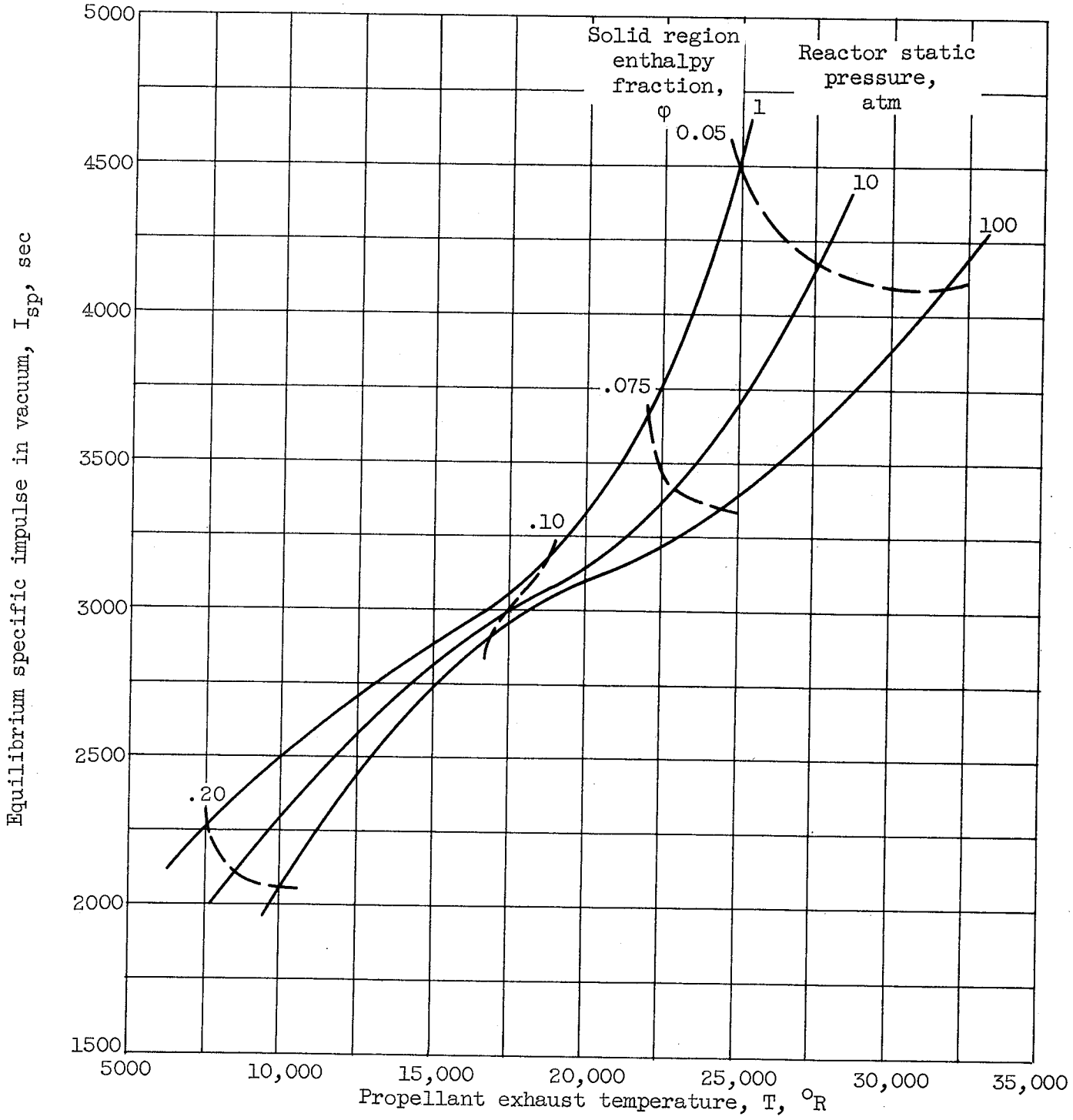

Figure 4. - Gaseous nuclear rocket specific-impulse - temperature relation as a function of reactor pressure and hydrogen enthalpy fraction gained in solid region at 5000° R inlet temperature.

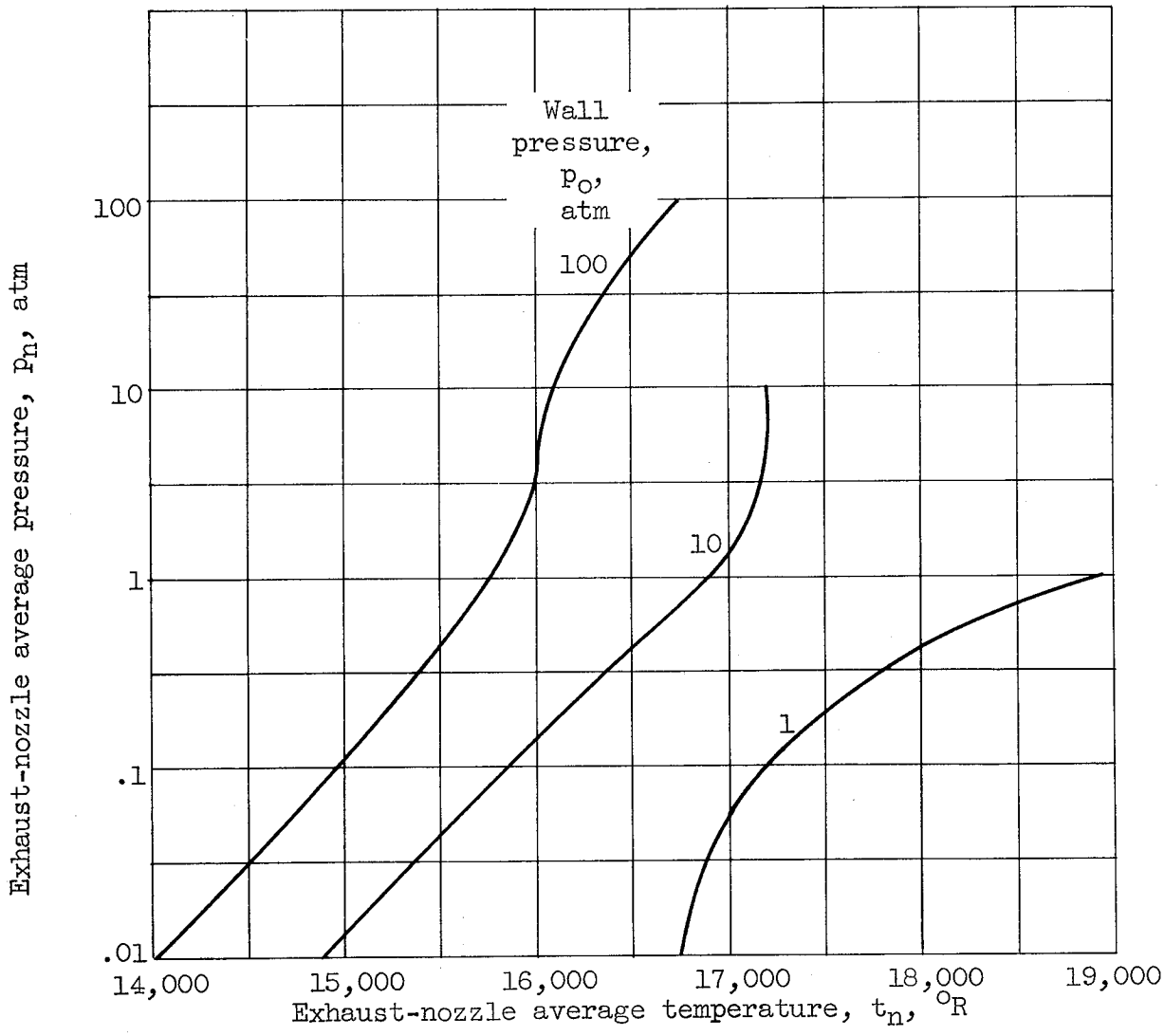

Figure 5. - Vortex exhaust-nozzle average pressure and temperature combinations to give enthalpy rise 10 times that of solid-core nuclear rocket with outlet gas temperature of 5000° R.

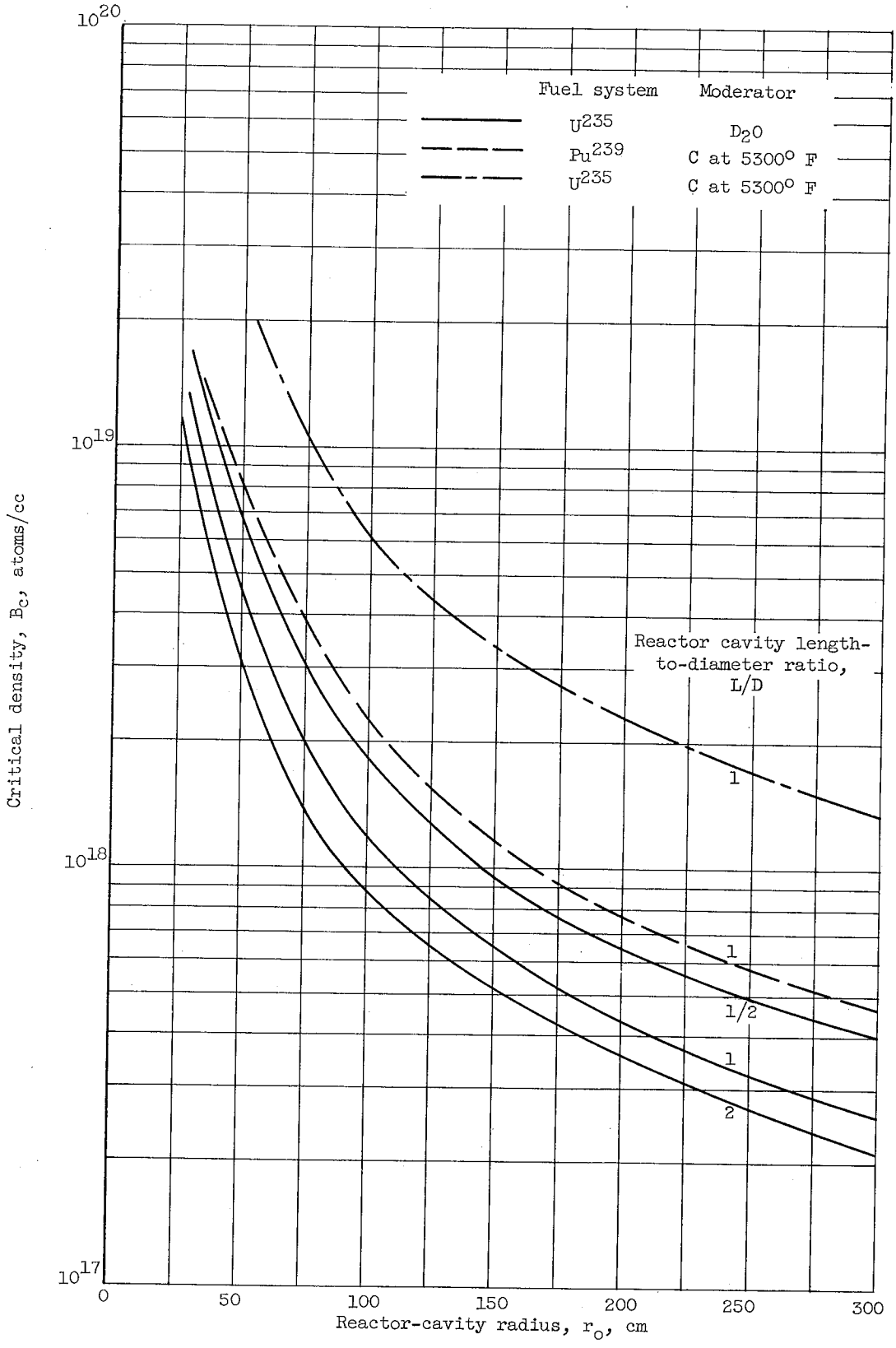

Figure 6. - Comparison of critical densities for three types of externally moderated cavity reactors.

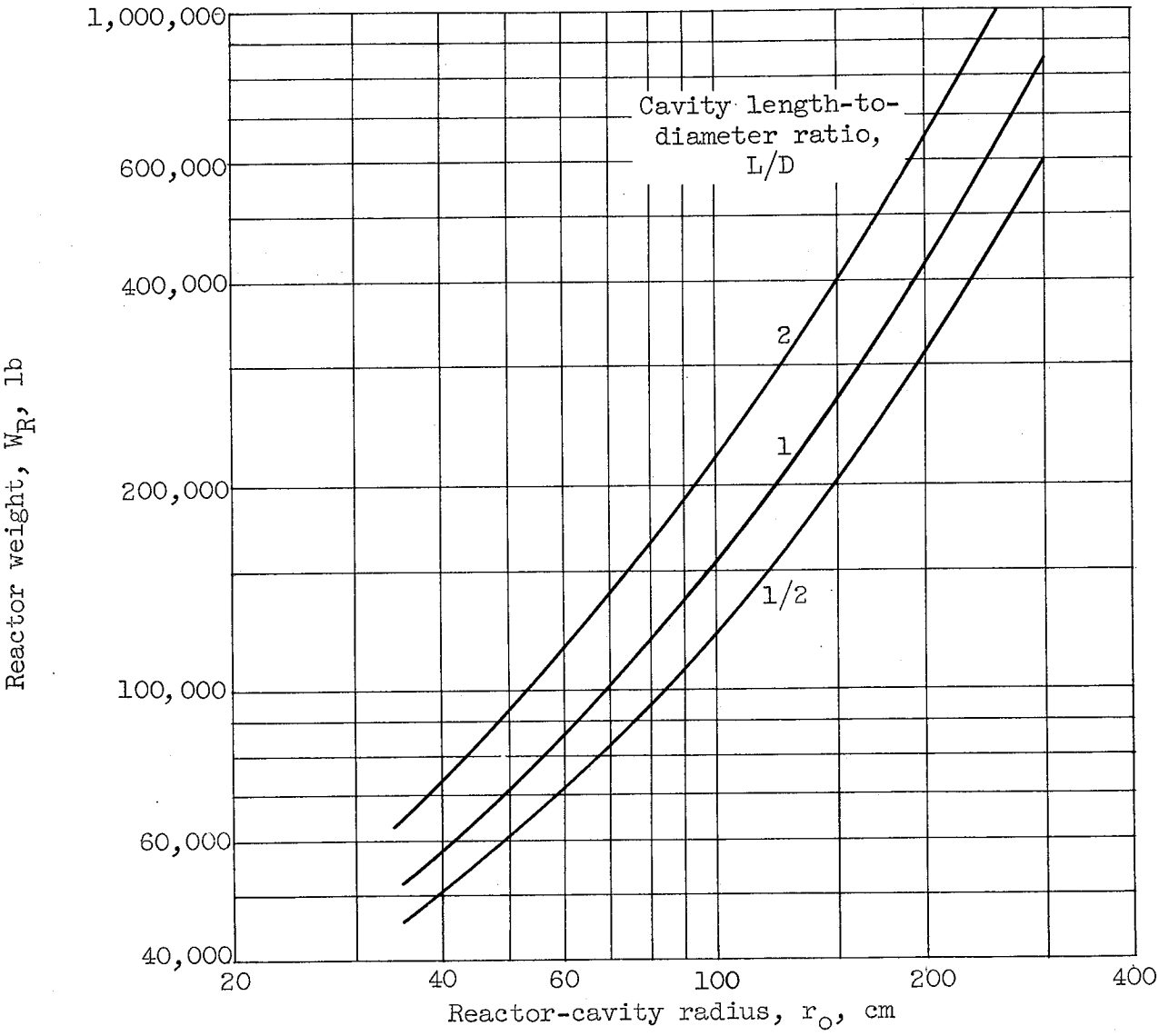

Figure 7. - Reactor (moderator) weight as a function of reactor-cavity radius and cavity length-to-diameter ratio. Moderator thickness, 100 centimeters.

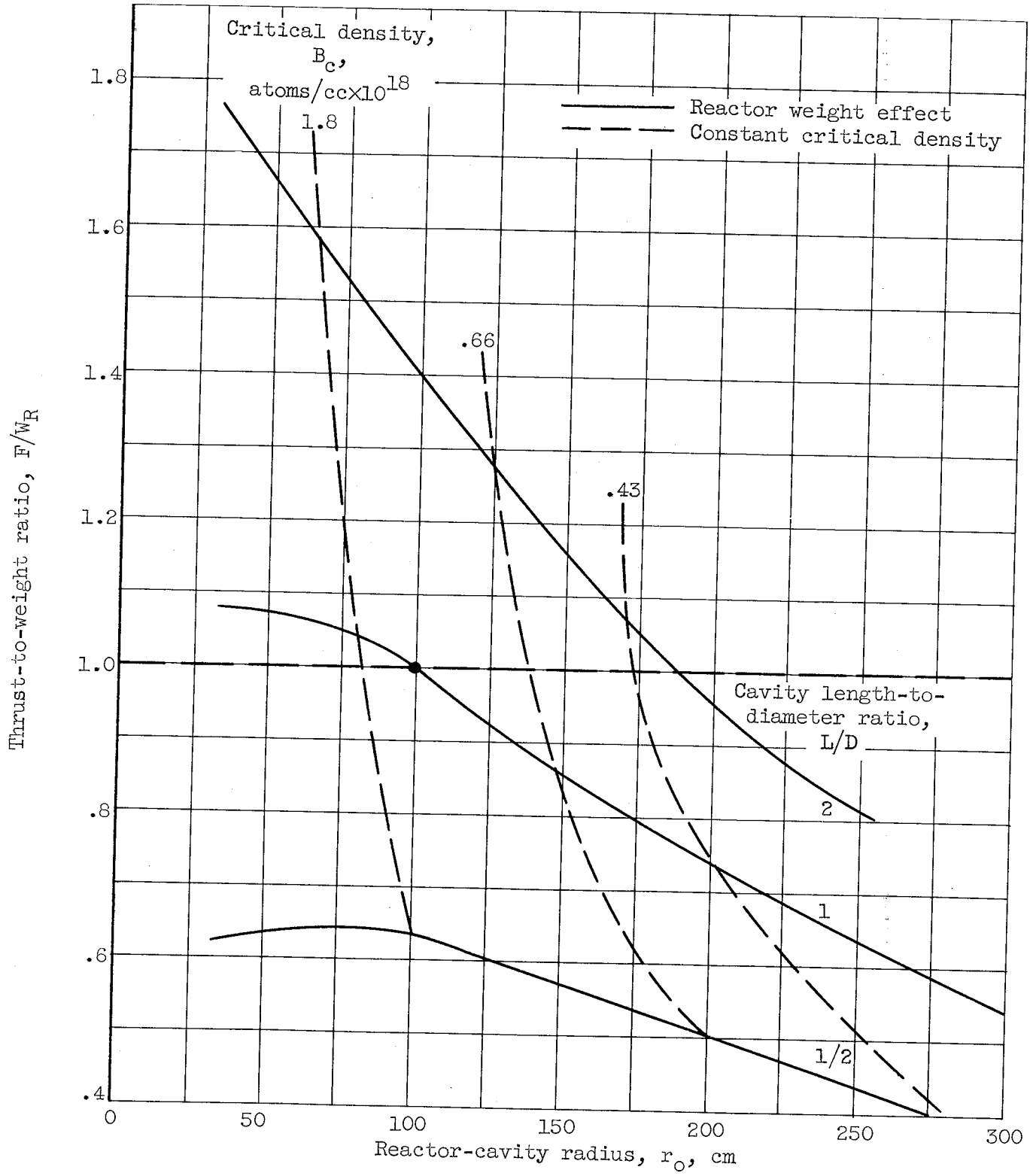

Figure 8. - Effect of reactor geometry on thrust-to-weight ratio normalized to reactor-cavity radius of 100 centimeters and a length-to-diameter ratio of 1 for constant specific impulse and propellant flow per unit length.

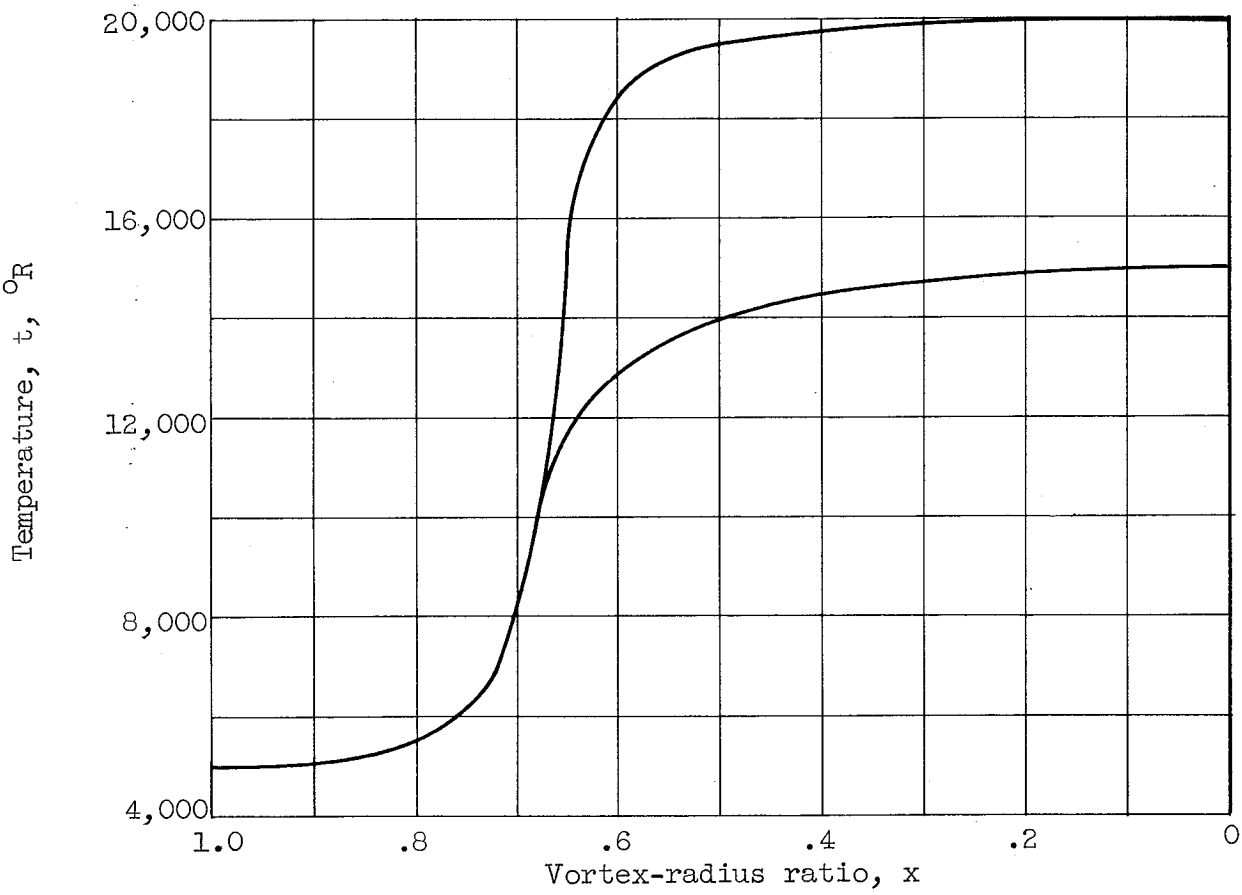

(a) Temperature profiles.

Figure 9. - Effect of temperature profile for laminar flow.

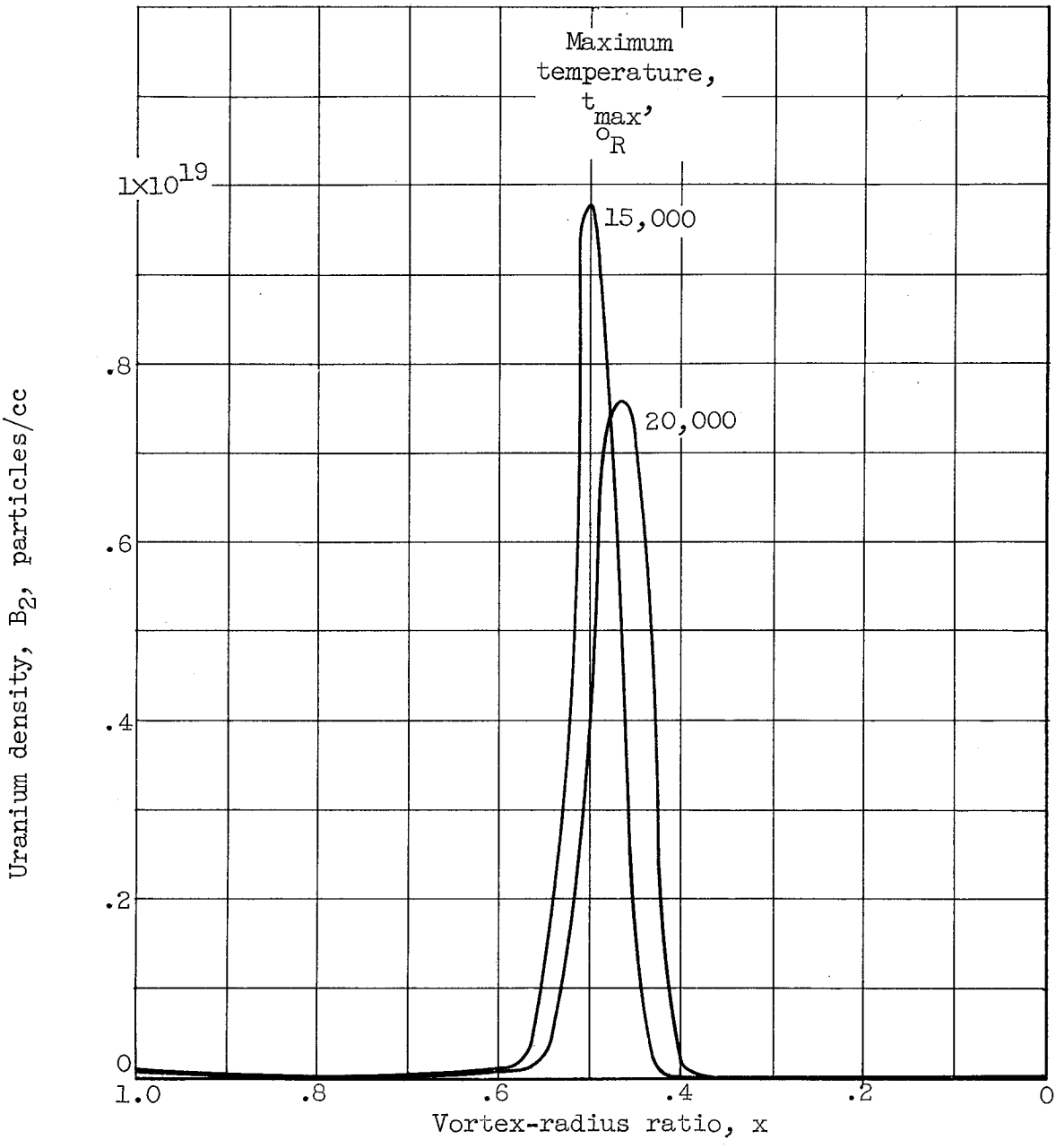

(b) Concentration profiles.

Figure 9. - Concluded. Effect of temperature profile for laminar flow.

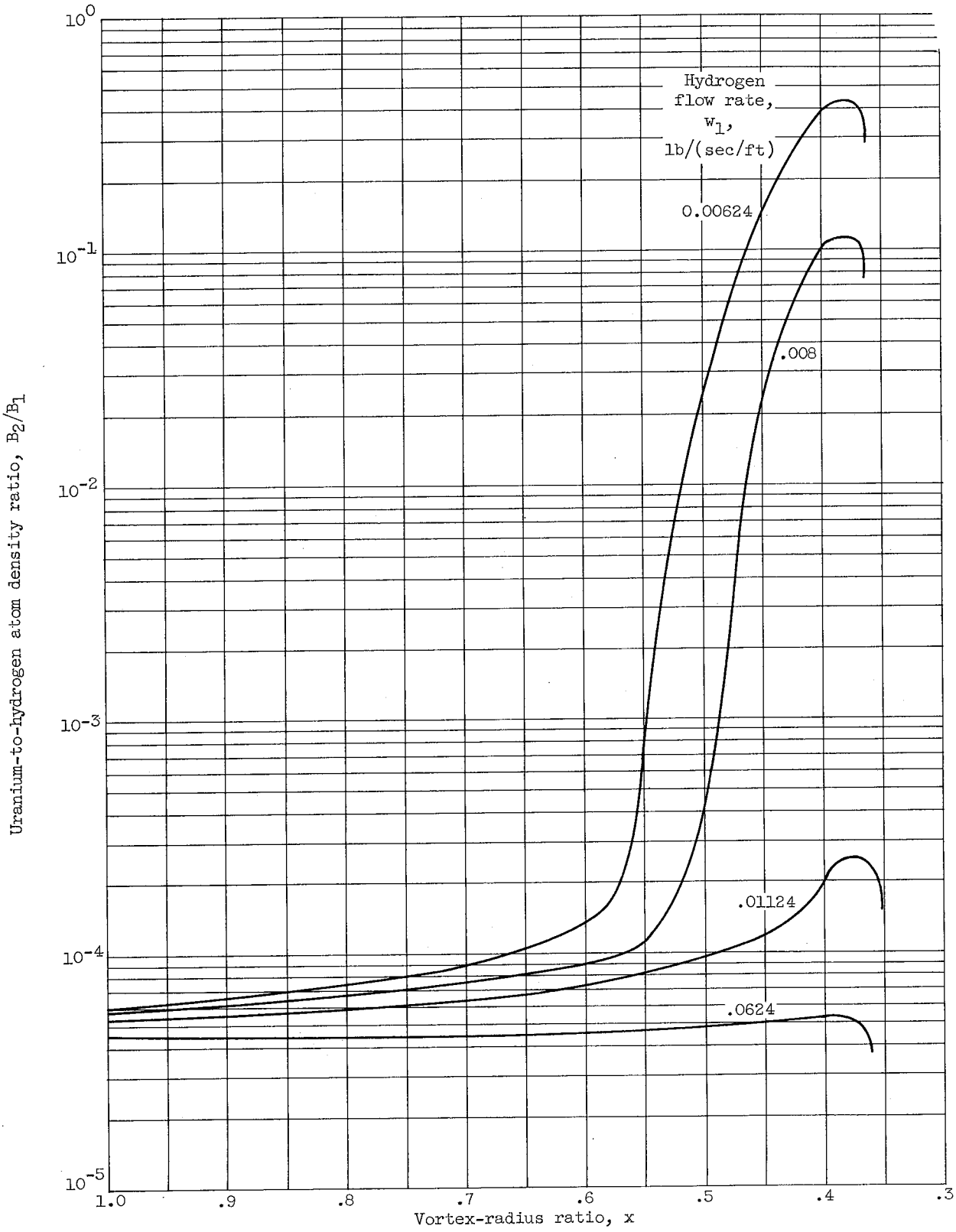

Figure 10. - Effect of hydrogen flow rate on separation for laminar flow. Hydrogen-to-uranium flow rate, 100; inlet static pressure, 500 atmospheres; inlet total temperature, 5000° R; peripheral Mach number, 0.9.

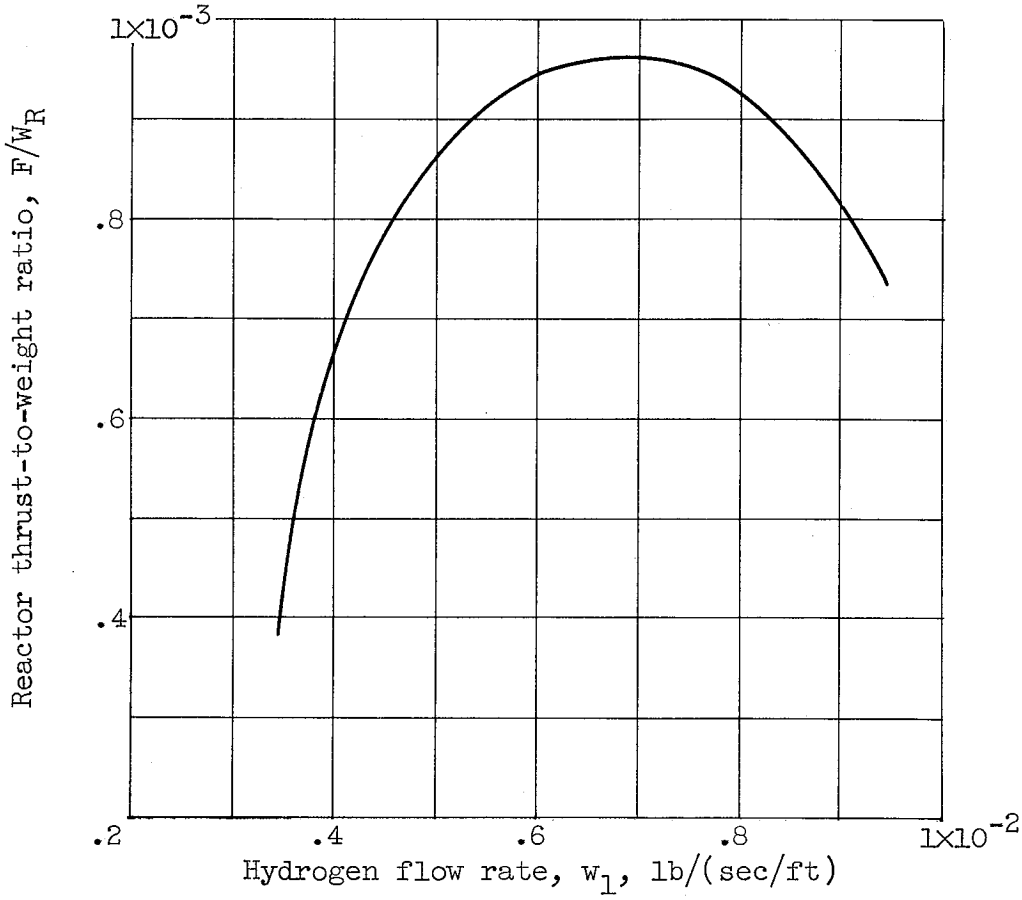

Figure 11. - Effect of hydrogen flow rate on reactor thrust-to-weight ratio for laminar flow. Hydrogen-to-uranium flow rate, 100; peripheral Mach number, 0.9; inlet static pressure, 500 atmospheres; inlet total temperature, 5000° R; reactor-cavity length-to-diameter ratio, 2.

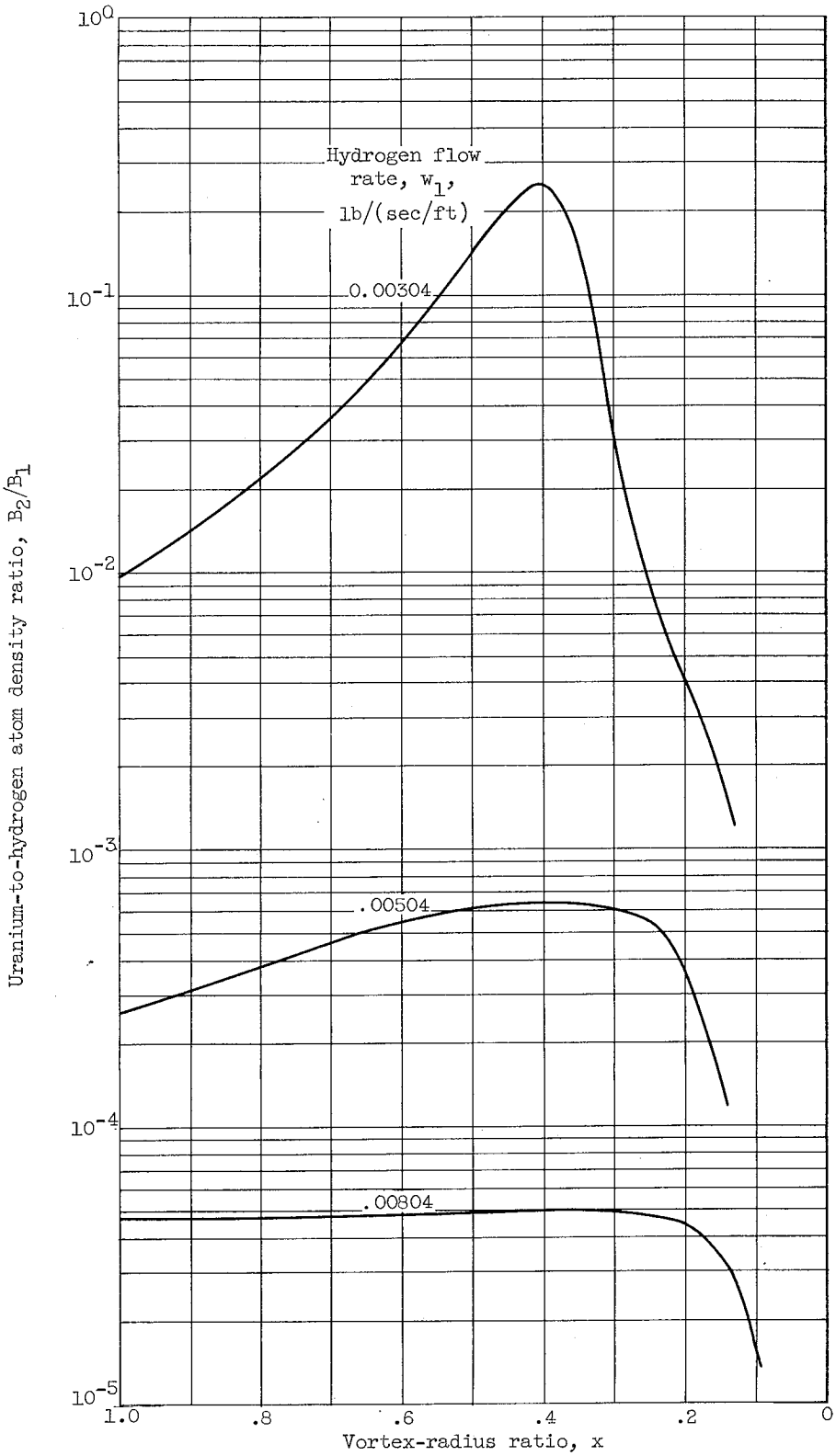

Figure 12. - Effect of hydrogen flow rate on separation for turbulent flow. Hydrogen-to-uranium flow rate, 100; inlet static pressure, 500 atmospheres; inlet total temperature, 5000° R; pheripheral Mach number, 0.9.

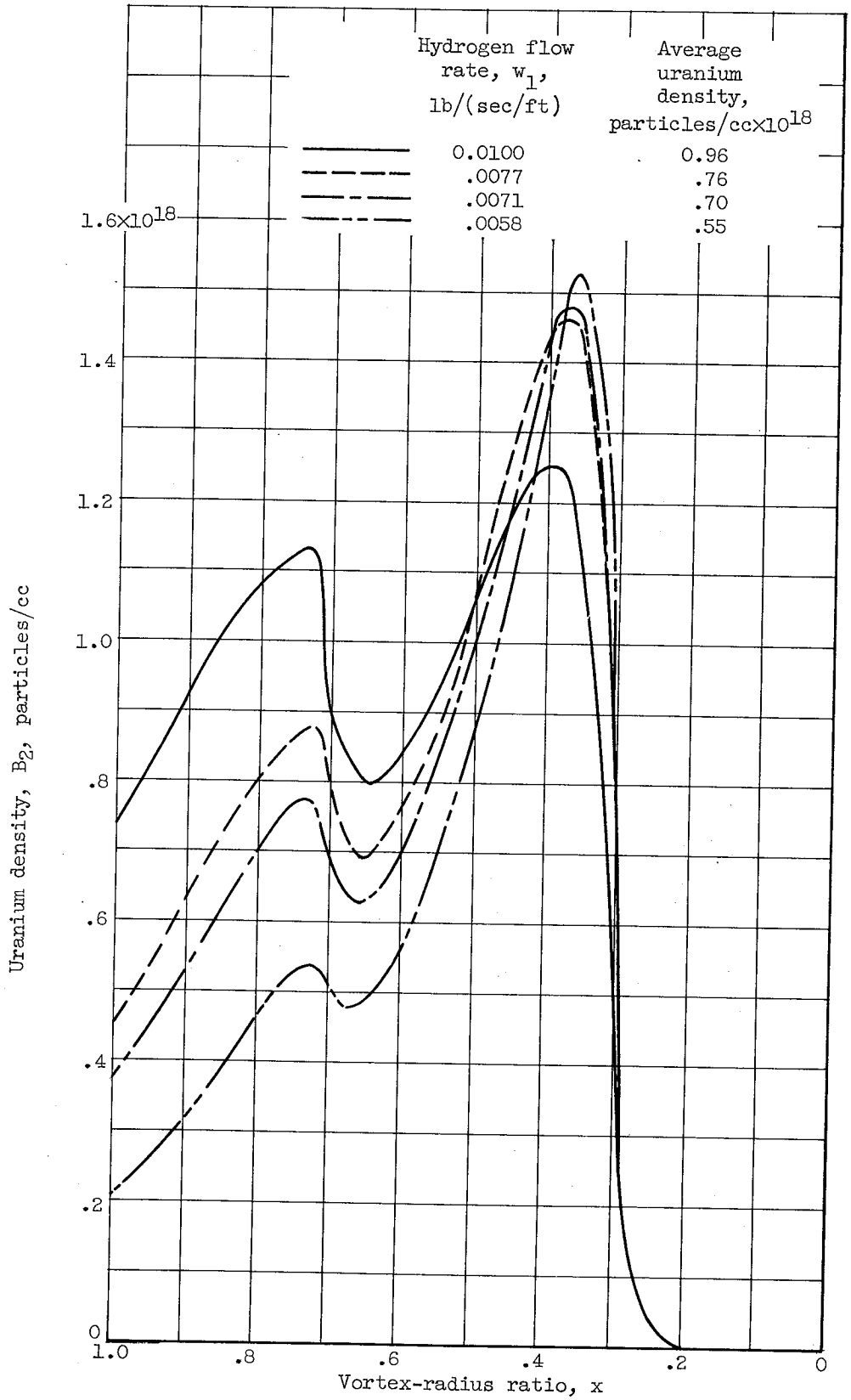

Figure 13. - Effect of hydrogen flow rate on uranium distribution for turbulent flow.

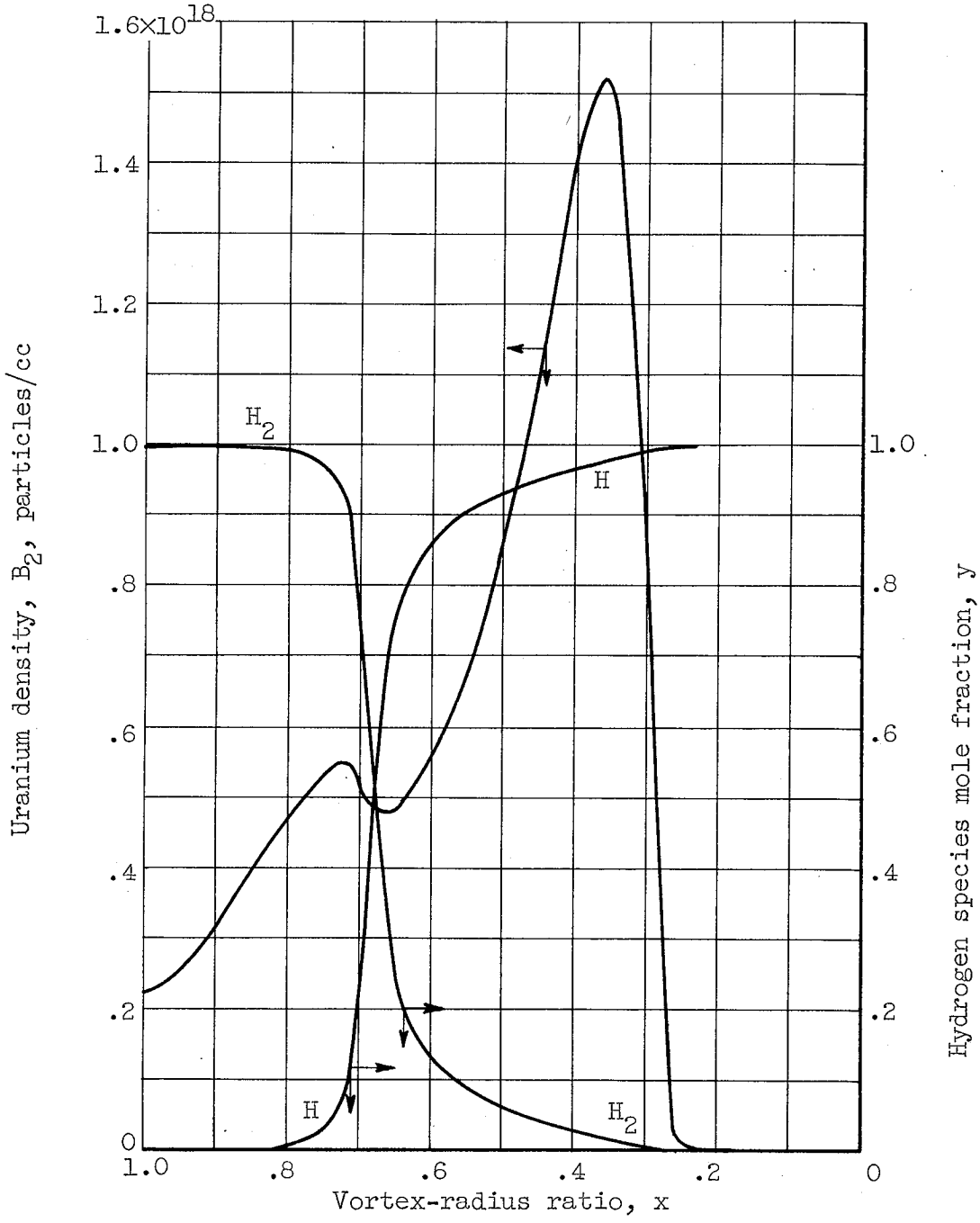

Figure 14. - Effect of dissociation on turbulent separation process.

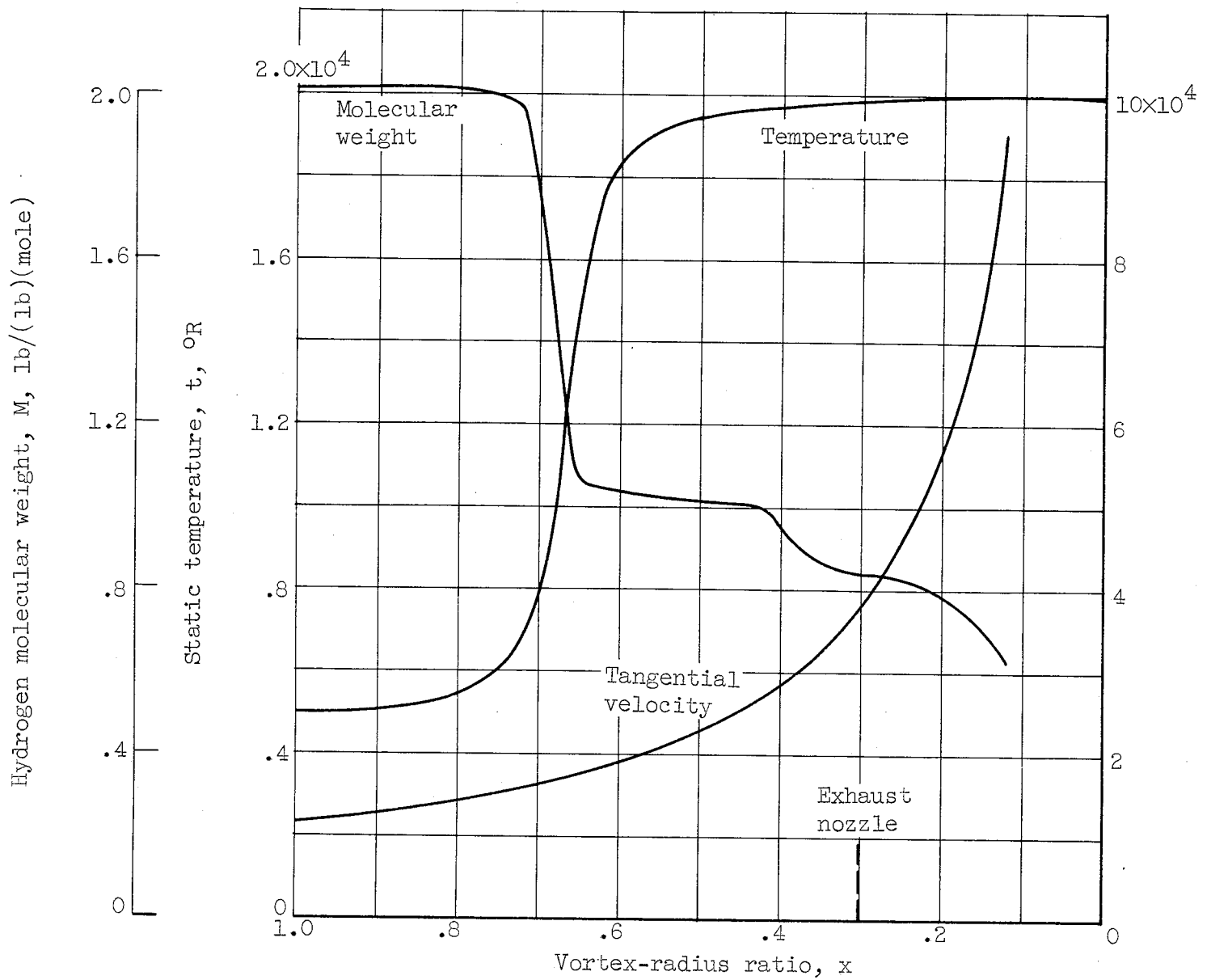

(a) Variation of tangential velocity, molecular weight, and static temperature.

Figure 15. - Illustrative laminar example.

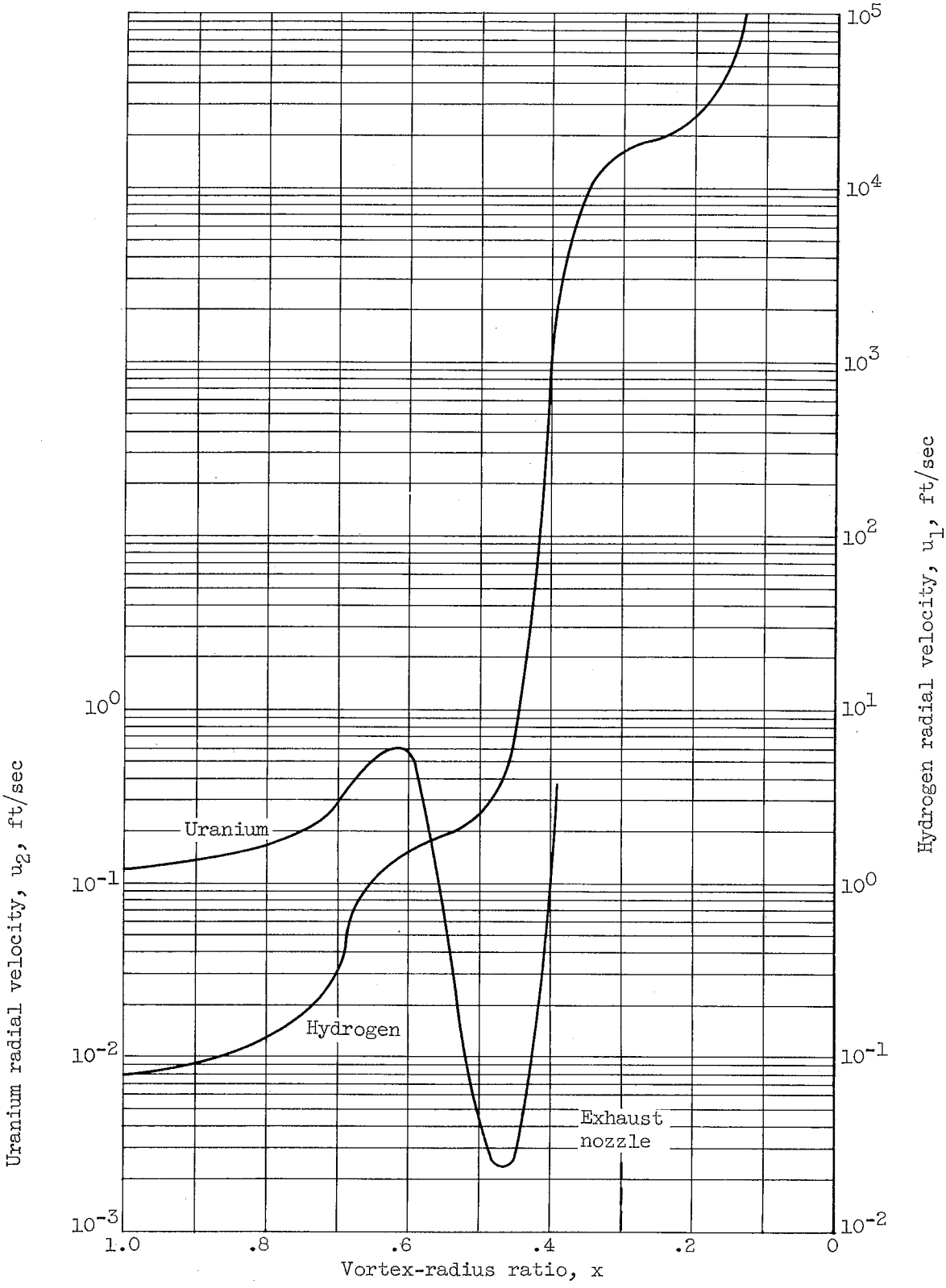

(b) Variation of species radial velocity.

Figure 15. - Continued. Illustrative laminar example.

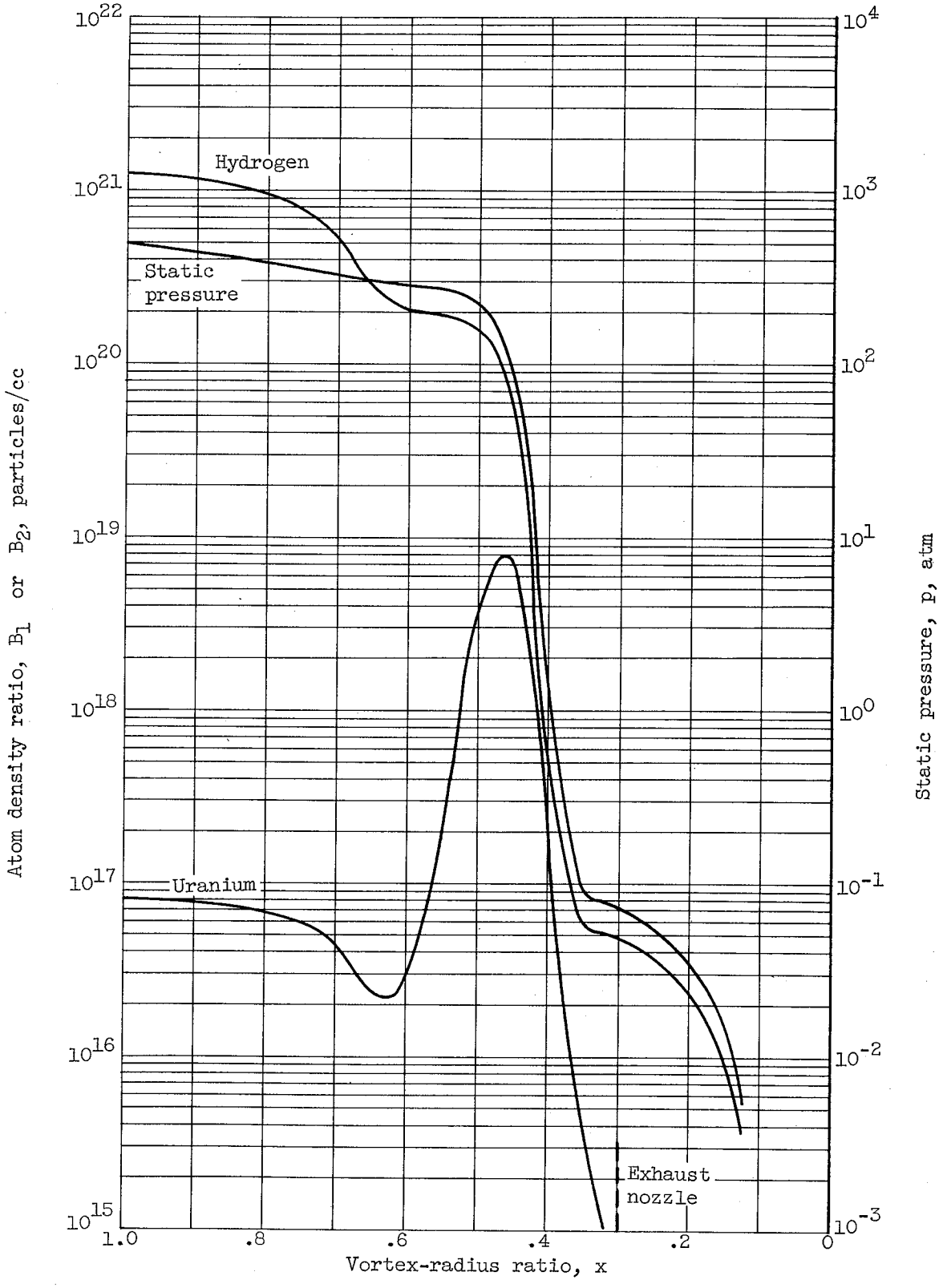

(c) Variation of species density and static pressure.

Figure 15. - Concluded. Illustrative laminar example.

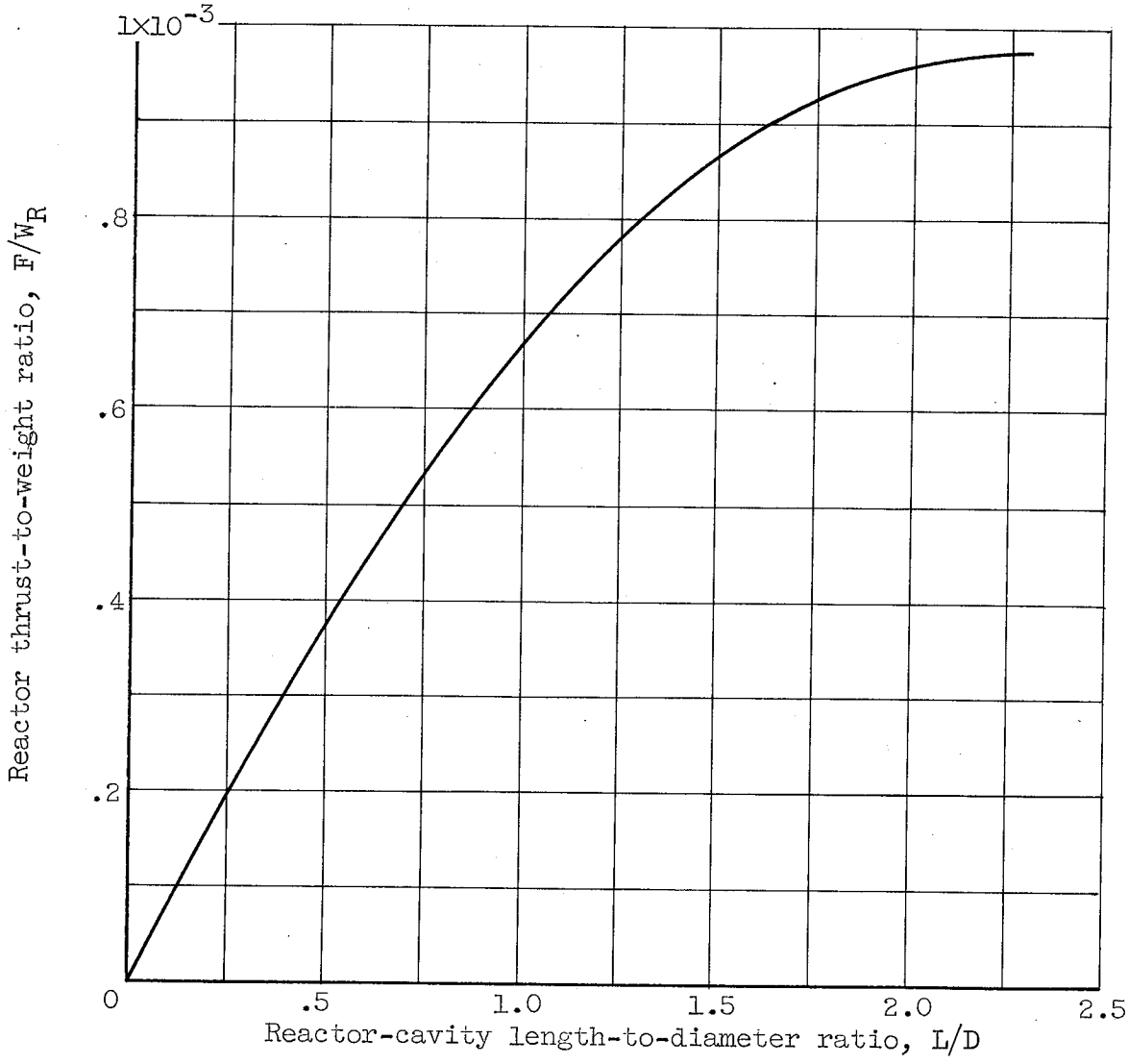

Figure 16. - Effect of reactor-cavity length-to-diameter ratio on reactor thrust-to-weight ratio for illustrative laminar example.

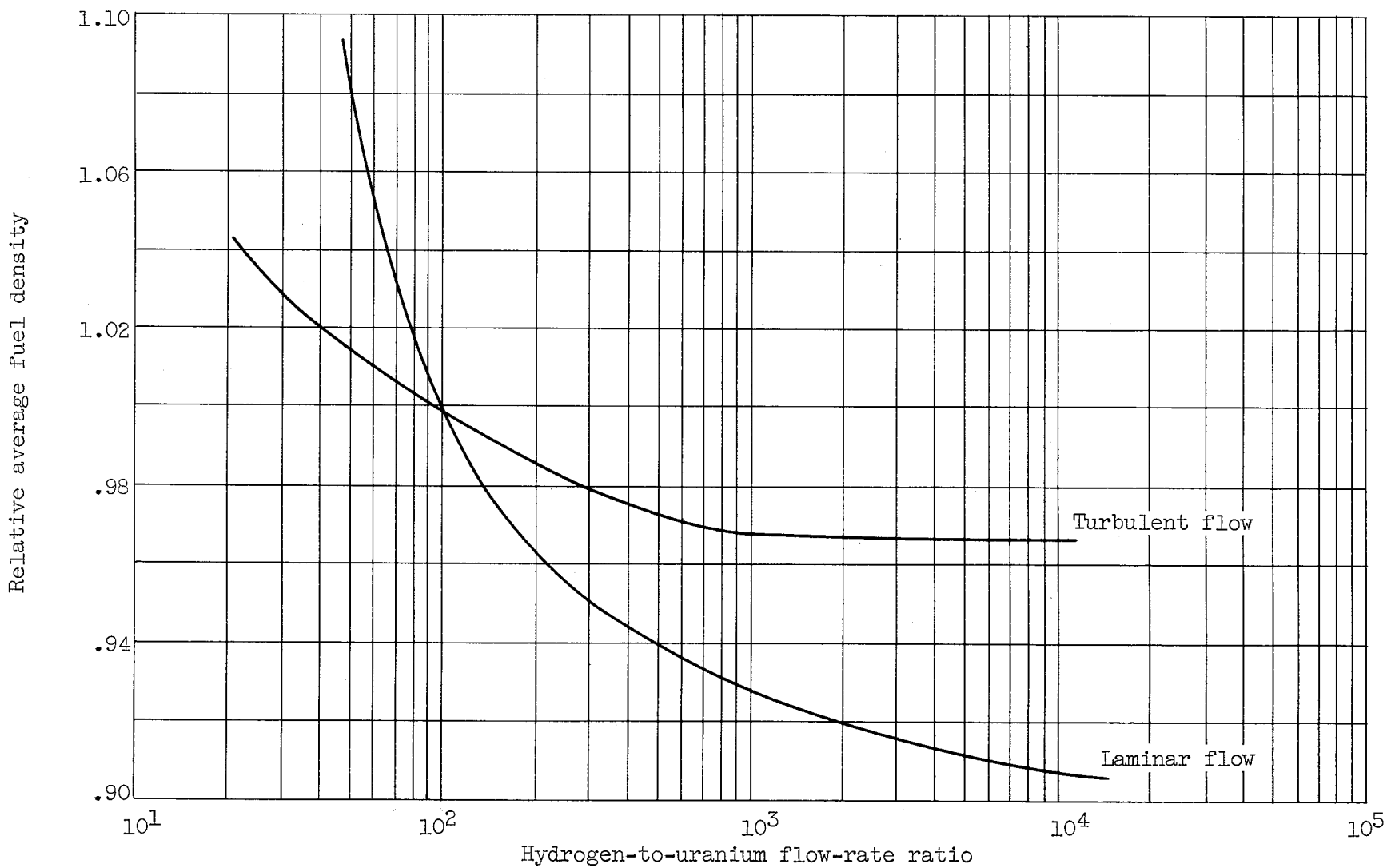

Figure 17. - Effect of hydrogen-to-uranium flow ratio on average fuel density.

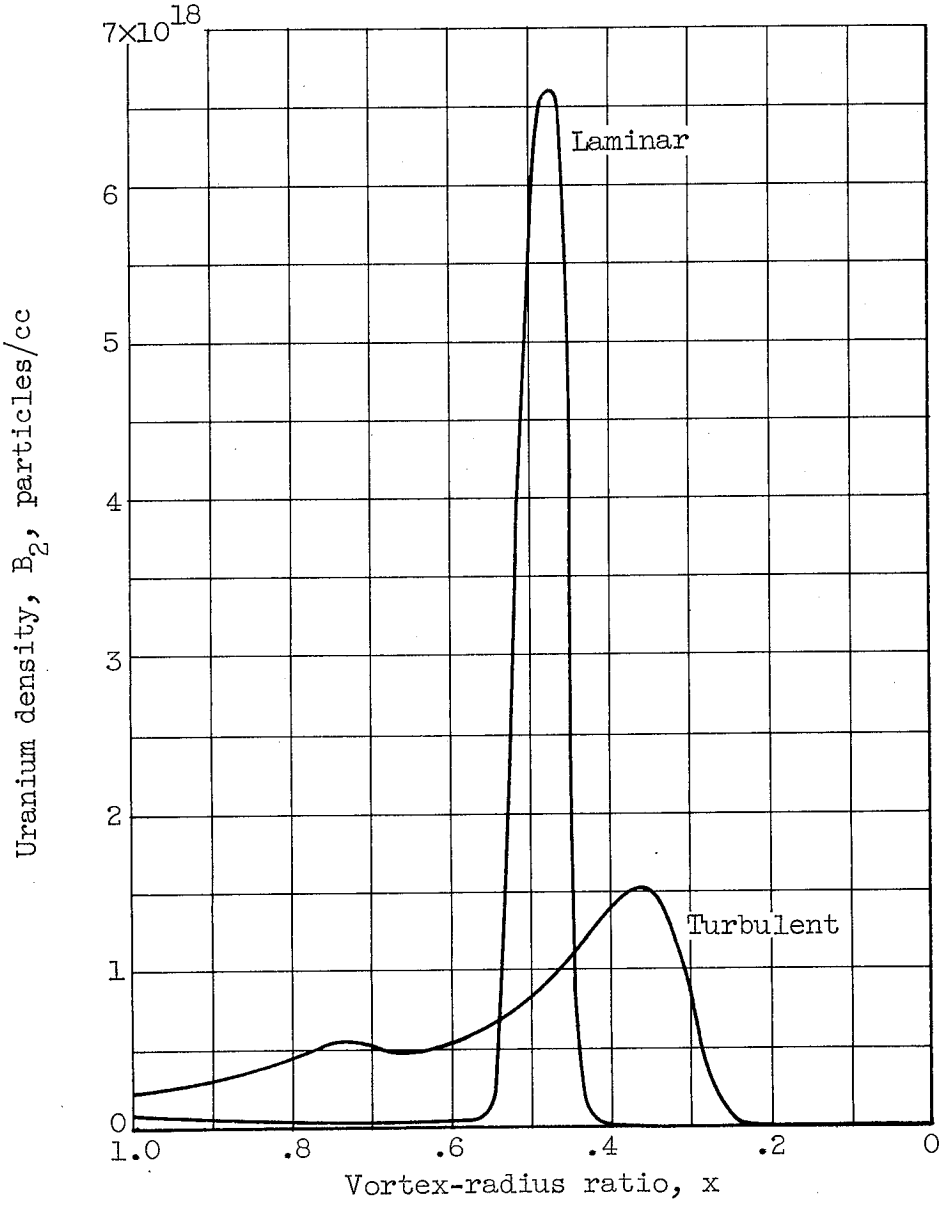

Figure 18. - Uranium-concentration profiles for best laminar- and turbulent-flow examples. Peripheral Mach number, 1; maximum temperature, 15,000° R; static pressure, 500 atmospheres; hydrogen-to-uranium flow ratio, 100.

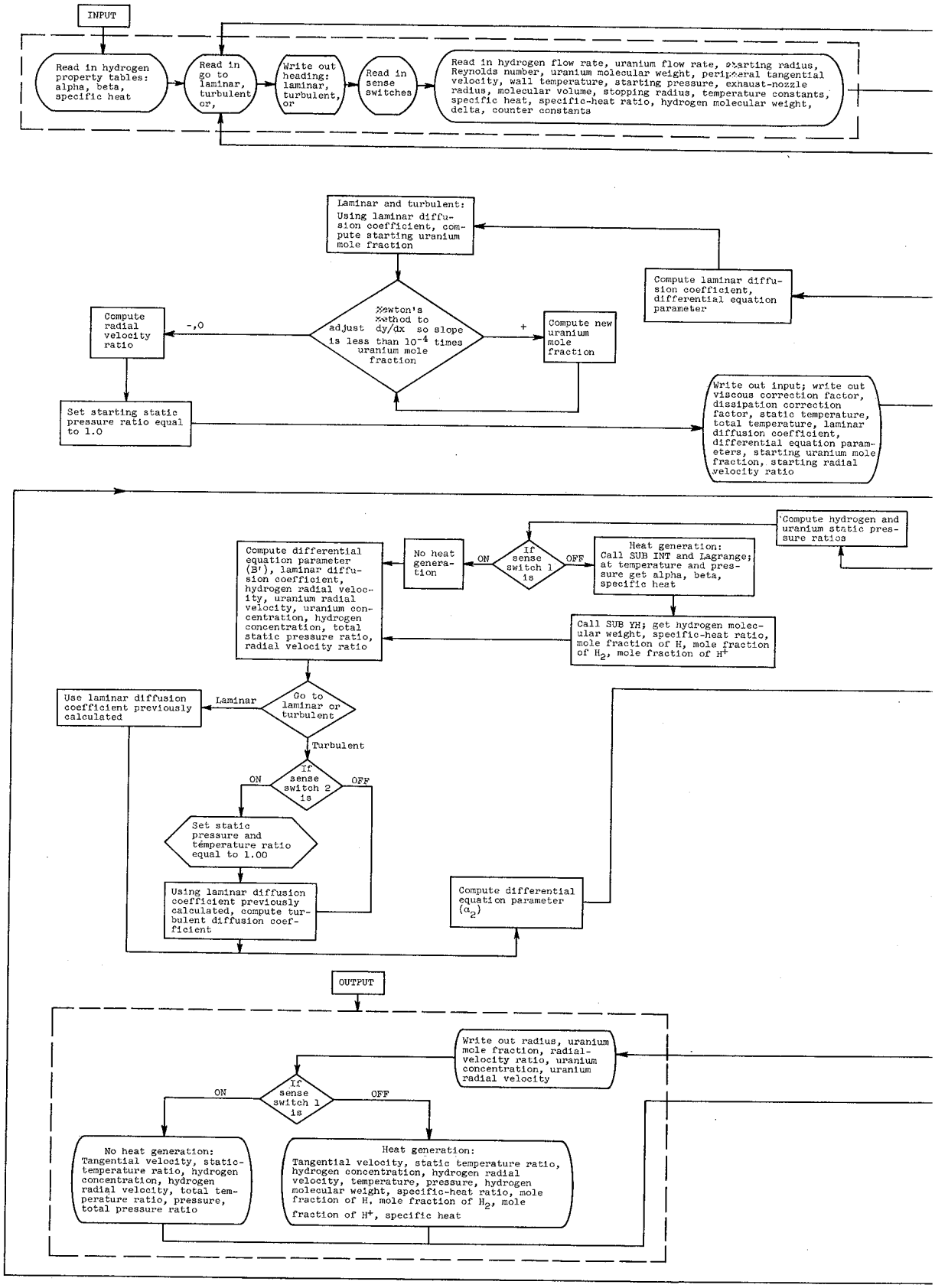

Figure 20. - Flow diagram of gaseou

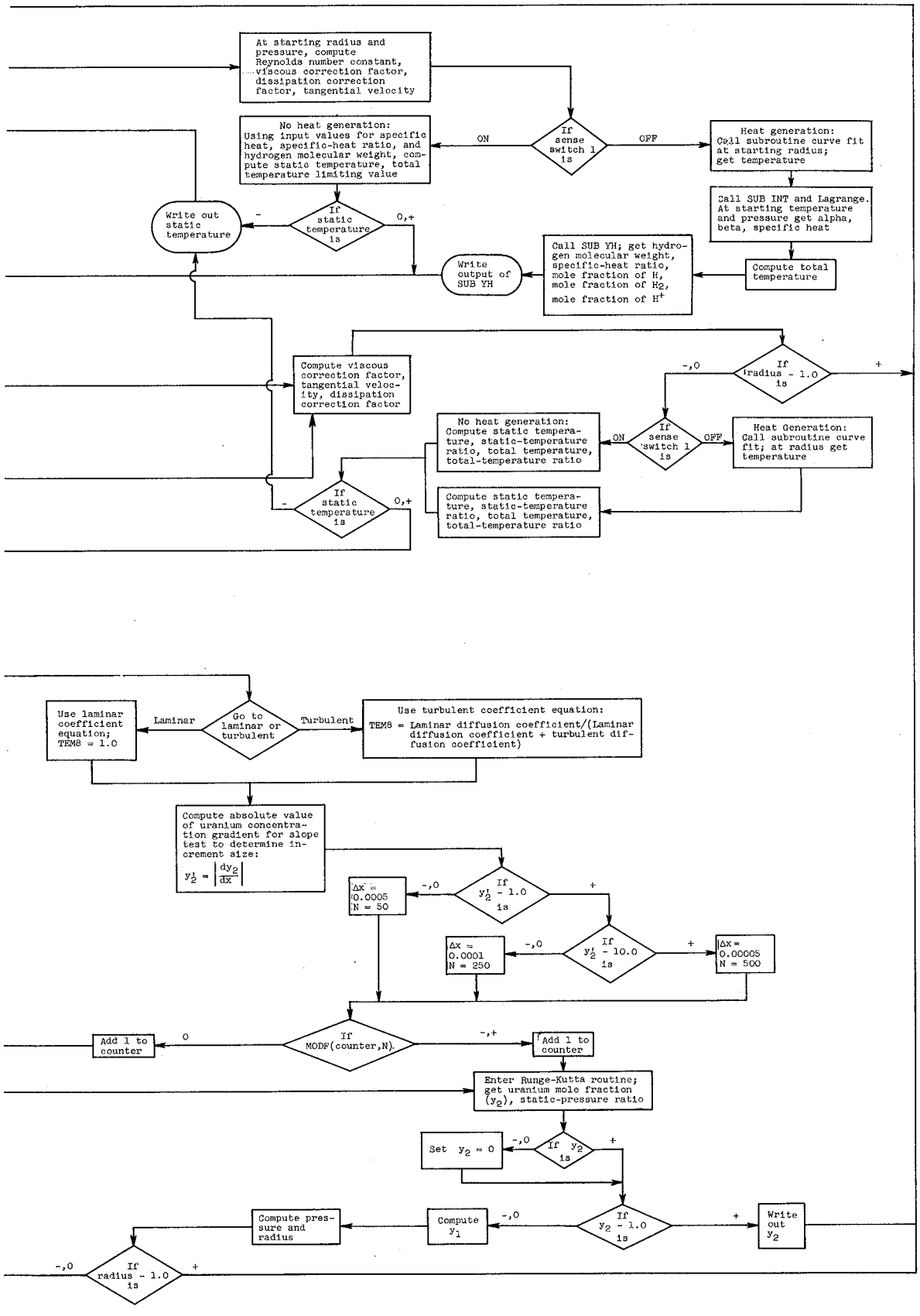

vortex-reactor hydrodynamic program.

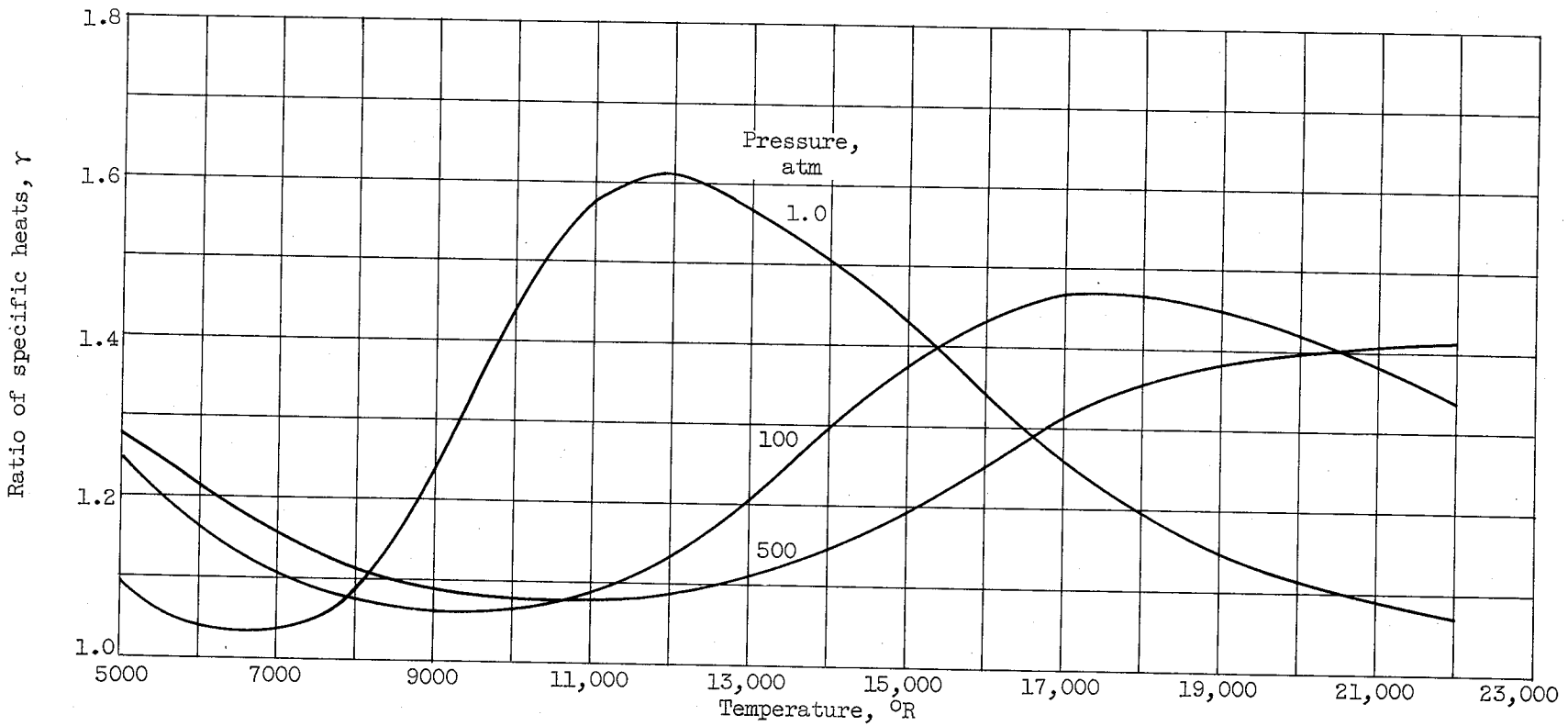

(a) Ratio of specific heats.

Figure 21. - Equilibrium properties of hydrogen gas.

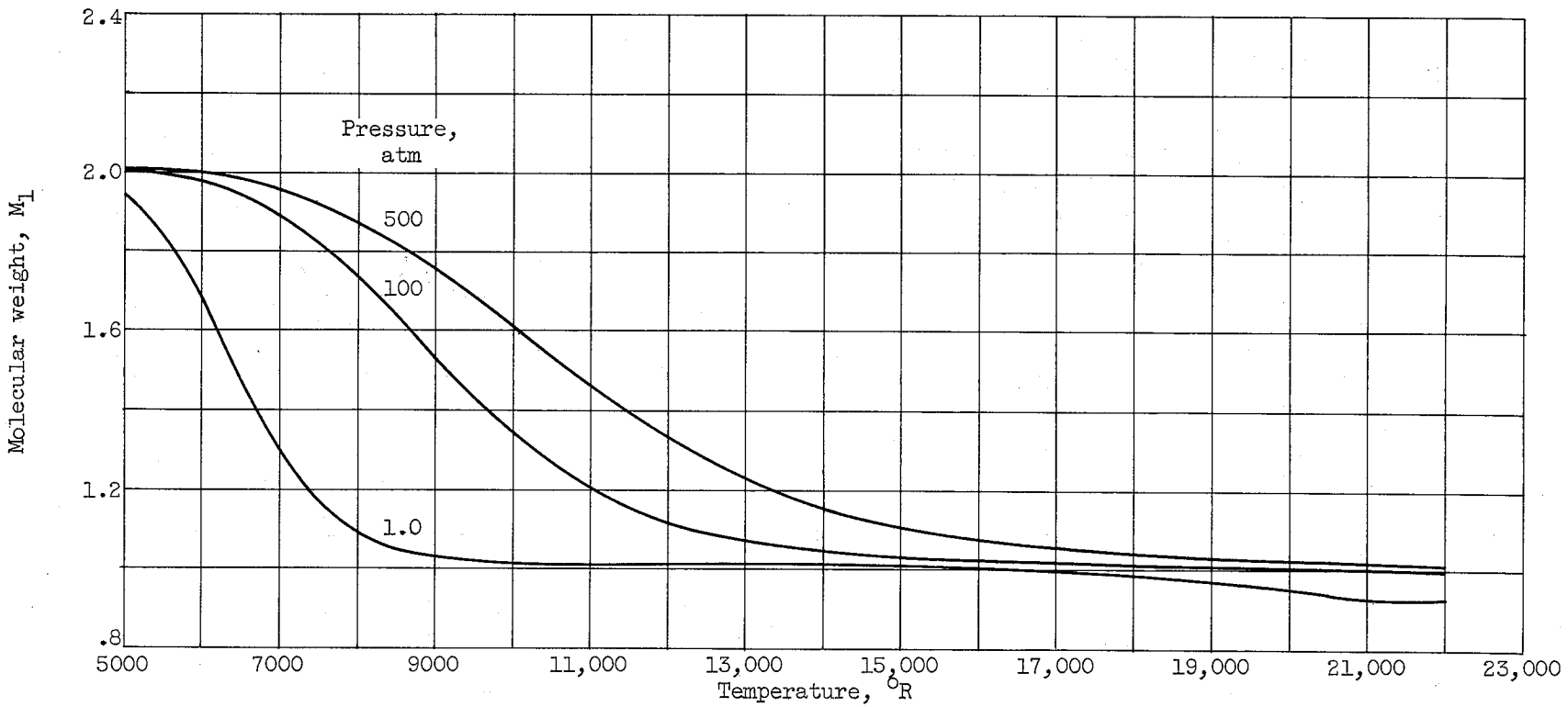

(b) Molecular weight.

Figure 21. - Continued. Equilibrium properties of hydrogen gas.

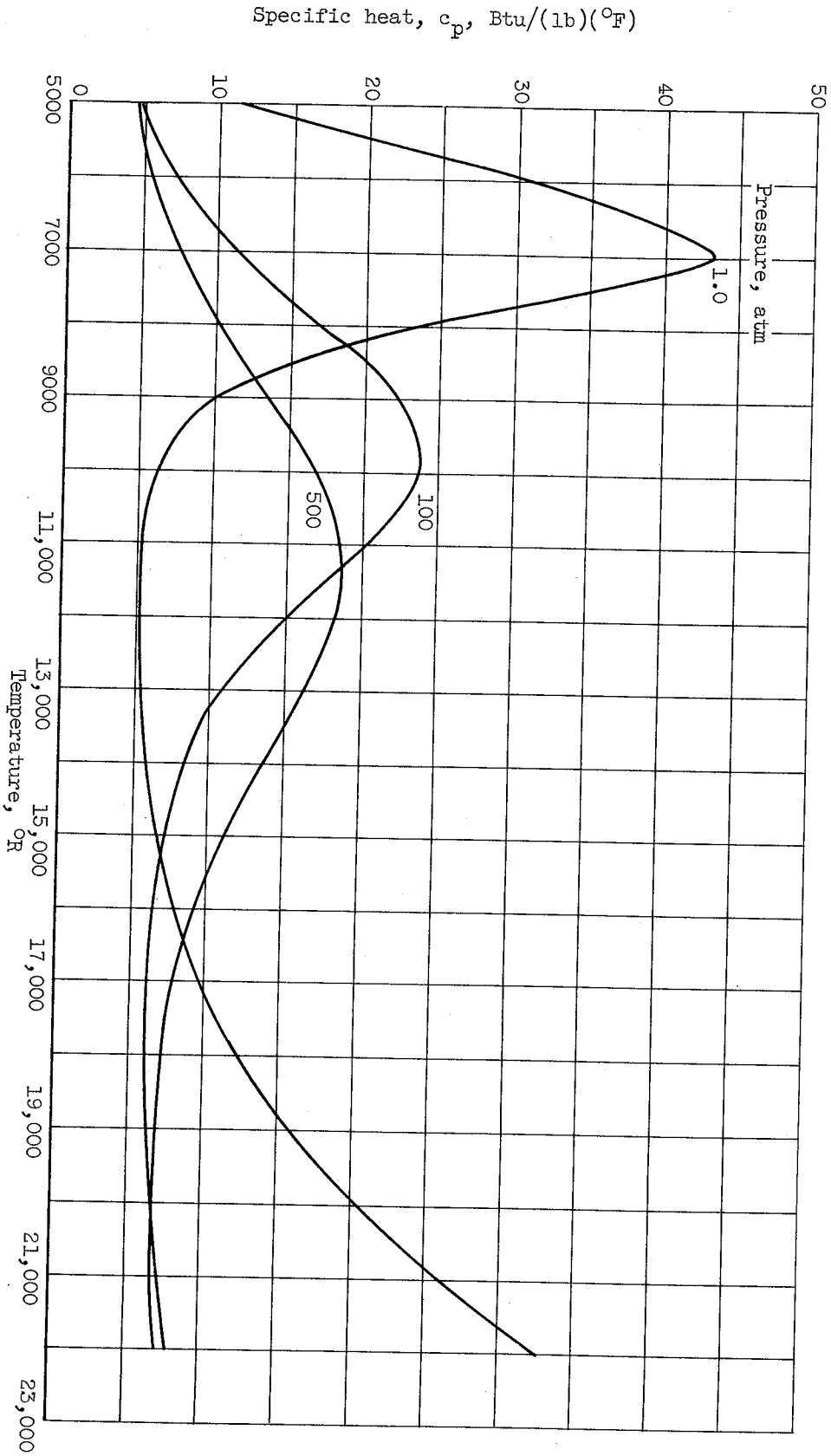

(c) Specific heat.

Figure 21. - Continued. Equilibrium properties of hydrogen gas.

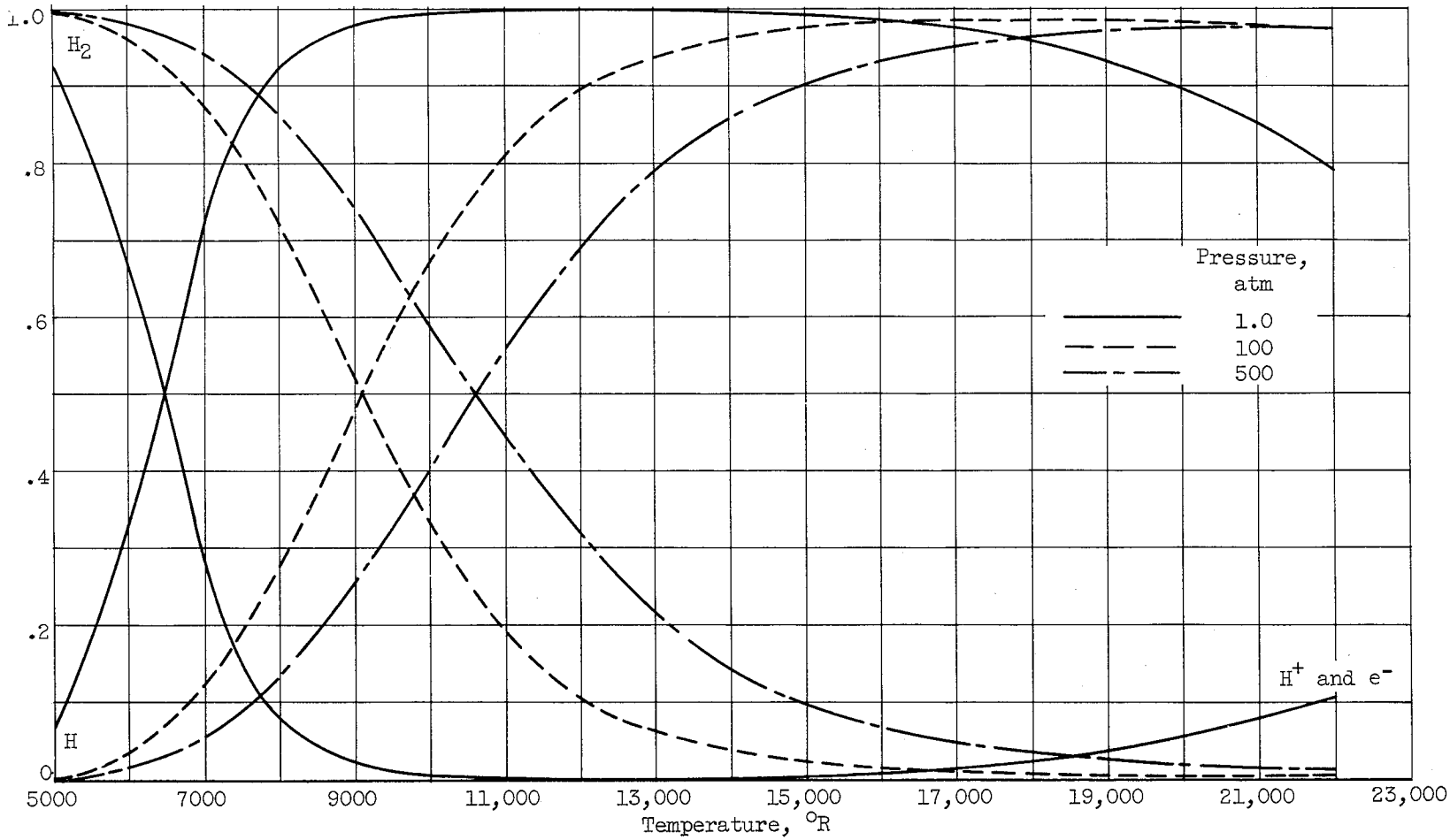

(d) Species concentrations.

Figure 21. - Concluded. Equilibrium properties of hydrogen gas.

NASA TN D-1579
National Aeronautics and Space Administration.
PERFORMANCE CAPABILITY OF SINGLE-CAVITY VORTEX GASEOUS NUCLEAR ROCKETS.
Robert G. Ragsdale. APPENDIX B: COMPUTER PROGRAM. Muriel B. Eian. May 1963. ii, 67p. OTS price, $1.75.
(NASA TECHNICAL NOTE D-1579)

A hydrodynamic analysis of two-component compressible vortex flow is used to determine hydrogen flow rates consistent with criticality requirements. Thrust per reactor weight is used as the criterion of performance, and a maximum value is determined for both laminar and turbulent flows. Hydrogen property variations are included in the hydrodynamic computer program that is described. The calculated variation of pertinent parameters with vortex radius is presented for a typical laminar example, and turbulence effects are discussed. Because of limits placed on hydrogen flow rate by the diffusion process, the performance capability of this system is less than that of an advanced solid-core nuclear rocket.

I. Ragsdale, Robert G.
II. Eian, Muriel B.
III. NASA TN D-1579

NASA

NASA TN D-1579
National Aeronautics and Space Administration.
PERFORMANCE CAPABILITY OF SINGLE-CAVITY VORTEX GASEOUS NUCLEAR ROCKETS.
Robert G. Ragsdale. APPENDIX B: COMPUTER PROGRAM. Muriel B. Eian. May 1963. ii, 67p. OTS price, $1.75.
(NASA TECHNICAL NOTE D-1579)

A hydrodynamic analysis of two-component compressible vortex flow is used to determine hydrogen flow rates consistent with criticality requirements. Thrust per reactor weight is used as the criterion of performance, and a maximum value is determined for both laminar and turbulent flows. Hydrogen property variations are included in the hydrodynamic computer program that is described. The calculated variation of pertinent parameters with vortex radius is presented for a typical laminar example, and turbulence effects are discussed. Because of limits placed on hydrogen flow rate by the diffusion process, the performance capability of this system is less than that of an advanced solid-core nuclear rocket.

I. Ragsdale, Robert G.
II. Eian, Muriel B.
III. NASA TN D-1579

NASA

NASA TN D-1579
National Aeronautics and Space Administration.
PERFORMANCE CAPABILITY OF SINGLE-CAVITY VORTEX GASEOUS NUCLEAR ROCKETS.
Robert G. Ragsdale. APPENDIX B: COMPUTER PROGRAM. Muriel B. Eian. May 1963. ii, 67p. OTS price, $1.75.
(NASA TECHNICAL NOTE D-1579)

A hydrodynamic analysis of two-component compressible vortex flow is used to determine hydrogen flow rates consistent with criticality requirements. Thrust per reactor weight is used as the criterion of performance, and a maximum value is determined for both laminar and turbulent flows. Hydrogen property variations are included in the hydrodynamic computer program that is described. The calculated variation of pertinent parameters with vortex radius is presented for a typical laminar example, and turbulence effects are discussed. Because of limits placed on hydrogen flow rate by the diffusion process, the performance capability of this system is less than that of an advanced solid-core nuclear rocket.

I. Ragsdale, Robert G.
II. Eian, Muriel B.
III. NASA TN D-1579

NASA

NASA TN D-1579
National Aeronautics and Space Administration.
PERFORMANCE CAPABILITY OF SINGLE-CAVITY VORTEX GASEOUS NUCLEAR ROCKETS.
Robert G. Ragsdale. APPENDIX B: COMPUTER PROGRAM. Muriel B. Eian. May 1963. ii, 67p. OTS price, $1.75.
(NASA TECHNICAL NOTE D-1579)

A hydrodynamic analysis of two-component compressible vortex flow is used to determine hydrogen flow rates consistent with criticality requirements. Thrust per reactor weight is used as the criterion of performance, and a maximum value is determined for both laminar and turbulent flows. Hydrogen property variations are included in the hydrodynamic computer program that is described. The calculated variation of pertinent parameters with vortex radius is presented for a typical laminar example, and turbulence effects are discussed. Because of limits placed on hydrogen flow rate by the diffusion process, the performance capability of this system is less than that of an advanced solid-core nuclear rocket.

I. Ragsdale, Robert G.
II. Eian, Muriel B.
III. NASA TN D-1579

NASA